Master in Computational Colour and Spectral Imaging (COSI)

Impact of LED Light Mixing on Color Discrimination in Low Vision

Master Thesis Report

Presented by

Linna Yang

and defended at the

Norwegian University of Science and Technology

September 2022

Academic Supervisor(s): Dr. Éric Dinet, Prof. Alain Trémeau, Dr. Pichayada Katemake

Jury Committee:

1. Dr. Giorgio Trumpy, Norwegian University of Science and Technology, Norway
2. Prof. Javier Hernández Andrés, University of Granada, Spain

Submission of the thesis: 10th August 2022
Day of the oral defense: 1st September 2022

Abstract

With the accelerated aging of the population, the number of people with low vision continues to rise. According to WHO, the majority of this group is beyond the age of 50, and 81 percent have never experienced a visual issue before. Visual impairment can have a significant impact on the quality of life and the ability of patients to live safely and independently. This study proposes an LED-based lighting strategy to aid those with age-related vision impairment. The methodology relies on psychophysical investigations using the arrangement of standard color samples. Under varying illumination conditions generated by a 24-channel multi-spectral lighting system, volunteers utilizing low vision simulation goggles performed this task. A filtering technique employing different color rendering indices and color measurements allowed for the objective determination of illumination conditions with the best color discrimination scores. The results of the experiment were utilized to combine three channels to produce white light that induces a stronger color perception in a low vision environment than the white LEDs currently used for general illumination. Even if further research is required, these preliminary findings offer hope for the development of intelligent lighting solutions that adapt to the visual needs of the visually impaired.

Acknowledgment

I would like to express my deepest gratitude to my supervisor Prof. Éric Dinet for his guidance. He trusted me, supported me, and encouraged me during all this work. I would also like to show my appreciation to Prof. Alain Trémeau, who gave me a lot of useful advice. I'm grateful to Prof. Philippe Colantoni, who generously provided knowledge and expertise, especially when I was facing problems. I also wish to acknowledge the help provided by Prof. Pichayada Katemake, who brought the color samples from Thailand to help me to catch up with the experiment.

Although this work did not go smoothly at first, with the light system broken twice, thanks to the active cooperation of Mr. Steve Paolini from Telelumen in the troubleshooting process, both incidents were well resolved. I also wish to extend my special thanks to all the participants in the psychophysical experiments. The experiments would not have been possible or carried out without their cooperation. Thanks should also go to the Hubert Curien Laboratory and Knowledge Center for Innovation at Jean Monnet University.

Thanks to the coordination of COSI joint master's degree program, Erasmus+ project and European Union for providing me with this opportunity and letting me have incredible two-year international experience in Norway, Spain, Finland, and France. I am also grateful to all the professors and lecturers in COSI for their high quality courses, which opened many doors to new knowledge for me. Many thanks to my classmates and all the cohort members. It is because they walked along with me together that made these two years shine!

Finally, I must express my very profound gratitude to my family and friends, who always support my decisions, always encourage me to discover different possibilities in life, always care about me, and always be my strong support as I continue to endeavor. Their belief in me has kept my spirits and motivation high during this work.

Yang Linna
Saint-Étienne, August 2022

Acronyms

AMD Age-related Macular Degeneration. 8–10, 21

ANOVA Analysis of variance. 39, 40, 42, 67, 69

AR Augmented Reality. 1, 9, 19

CCT Correlated Color Temperature. 10, 11, 13, 20, 46, 47

CER Circadian Efficacy of Radiation. 15

CES Color Evaluation Samples. 13, 14

CIE International Commission on Illumination. 11, 14, 36, 43, 46

CLE Circadian Luminous Efficacy. 15

CQS Color Quality Scale. 14, 31, 32, 52, 67

CRI Color Rendering Index. 13, 14, 31, 32, 46

CVG Color Vector Graphics. 33, 67

ETA Electronic Travel Aid. 17, 18

FWHM Full Width at Half Maximum. 22, 24

GAI Gamut Area Index. 15, 47

GPS Global Positioning System. 18

HMD Head Mounted Device. 9, 19, 20

HVS Human Visual System. 3, 4, 21

ICD-11 International Classification of Diseases 11th Revision. 6

IES Illuminating Engineering Society. 14, 24

IR Infrared. 23

LED Light-Emitting Diode. 1, 2, 10, 13–15, 21, 22, 24, 32, 35, 43, 46, 49, 50

LGN Lateral Geniculate Nucleus. 3

MR Mixed Reality. 19

NCS Natural Color System. 36, 47

NIF Non-Image Forming. 10

NIST National Institute of Standards and Technology. 14

SI International System of Units. 11, 13

SPD Spectrum Power Distribution. 20, 23

UGR Unified Glare Rating. 10, 15

UV Ultraviolet. 23

VA Visual Acuity. 3, 6, 25, 36

VR Virtual Reality. 9

Contents

1 | Introduction

1.1 Problem Statement

The number of people over 65 years old will double by 2050(WPP, 2019). And it is estimated that the 60+ age group population will increase to 21.8% in 2050 and nearly one-third in 2100 (Lutz et al., 2008). This aging trend may cause many social and health problems. Since aging is one of the main factors for many visual impairments (Wong et al., 2014; Tham et al., 2014), it is very important to propose a vision support method to help people suffering from deteriorating eye conditions to use their remaining vision in order to assist them in their daily activities.

Unlike the other traditional visual assistive methods such as smart cane or some recent solutions based on Augmented Reality (AR) glasses, the Light-Emitting Diode (LED) lighting approach offers many advantages as a visual aid: the world representation of low vision people is not changed; the field-of-view is unlimited; no device has to be worn which preserves natural movements; both hands are free to perform more easily daily activities; the lighting conditions can be adapted to the visual environment as well as to the visual deficiency reducing by the way the rehabilitation constraints. Moreover, the residual vision is still stimulated, which is highly recommended by all professionals working in the field of low vision. By exploiting the color capabilities and the tuning range of LED-based lighting systems, important elements are available to achieve a low vision aid which can be personalized and set up for different visual impairments.

1.2 Scope and Aims

This report focuses on the study of color discrimination in one typical visual impairment — central loss vision — among the age-related eye degeneration to investigate the effects of LED light mixing to increase the color difference to help people with low vision achieve better visual performance. The proposed method is designed for people who still have functional vision but with mild to middle degeneration, especially due to aging. People with congenital eye diseases and people with severe vision deficiency need more specialized medical care, so these people are not in the target study scope.

Also, the colors in daily life are varied, with different appearances and materials. To control the experiment variables, this research abstracts the hue as the only variable to conduct the experiment. The glossary, texture, and translucency of the appearance are not included in this study.

This study seeks to identify the ideal LED mix spectrum that can assist and enable low-vision individuals to distinguish colors more quickly and easily, hence facilitating their daily tasks. Also, it is worthwhile to analyze and draw conclusions regarding the various illumination characteristics for future research. Therefore, the main experimental procedure includes two phases: optimization of the LED light mixing and the validation of the proposed lights. The structure of this report is as mentioned below.

1.3 Structure of this Thesis

Chapter 2: The theoretical background information related to this research.

Chapter 3: The literature review in the related field.

Chapter 4: The investigation process of this research. (Phase I)

Chapter 5: The validation and testing process of the outcomes. (Phase II)

Chapter 6: Discuss some details or the observations.

Chapter 7: An overall conclusion and the possible future work.

2 Background

This chapter contains an overview of concepts related to human color perception, low vision, and lighting property. This background information is provided for a systematic understanding of the experiments.

2.1 Human Color Perception

2.1.1 Human Visual System

The Human Visual System (HVS) encompasses the eyes, optic nerves, Lateral Geniculate Nucleus (LGN), visual cortex, and all connecting pathways between them. Each component of the HVS is indispensable for proper vision, and each part has its own essential functions in this complex system.

For the eyes, as the exposed organ of the visual system, there are many risk factors that can affect their condition, including but not limited to genetics, physical damage, and aging. Figure 2.1 shows the anatomical structure of human eyes. The eye is a very delicate optical system. It first collects light from the environment, adjusts the intensity of the light entering the eye through the iris, uses an adjustable lens to focus, and projects an image onto the light-sensitive retina, which is then converted into an electrical signal and transmitted to the brain via the optic nerve.

However, the final image we "see" may vary from person to person due to the differences in visual conditions. Visual Acuity (VA) is a clinical measure that describes the clarity of human vision and indicates how well the eyes are functioning. The value of VA includes 2 digits. For example, 6/12 means the observer is able to see as well at a distance of 6 meters as an average person sees at a distance of 12 meters. Additionally, the scale can be expressed in either meters or feet, depending on the country. The standard distance for the Snellen chart (the eye chart used to measure VA) is 6 meters (or 20 feet), so the normal VA 6/6(m) is equivalent to 20/20(ft). In this report, all VAs are expressed in meter system.

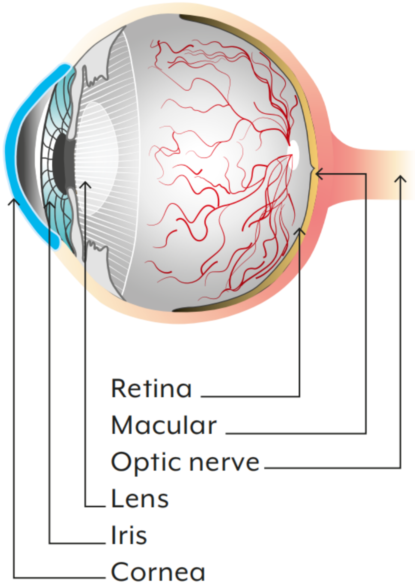

Figure 2.1: *Human eye structure (WHO, 2019)*

2.1.2 Color Vision Theories

HVS is also able to distinguish different colors, or in other words, having color perception. Nowadays, there are two predominant theories about color vision: the trichromatic theory and the opponent process theory.

Trichromatic theory is based on the three types of cone receptors in the human retina, namely the L-cone, M-cone, and S-cone receptors, which roughly correspond to the highest sensitivity for red, green, and blue. This theory can be traced back to the 19th century and is also called the "Young-Helmholtz theory", since Thomas Young and Hermann von Helmholtz conducted psychophysical work on color matching in the 1800s. One of the empirical evidence is that any color has the probability of being mixed by three different wavelengths of light. The trichromatic theory assumes that all wavelengths of color can be signaled by the activity of three classes of photoreceptors and transmit the signal to the visual cortex of the brain (Baraas et al., 2018).

Opponent process theory was first proposed by Ewald Hering in late 1800s. This theory is based on many subjective observations. One important phenomenon is the color afterimages, which cannot be explained by the trichromatic theory. Another observation is that it is not possible to perceive reddish-green or bluish-yellow. These facts provide the clue of opponent vision processing, the red-green, yellow-blue, black-white are the three primary opponent pairs. Opponent process theory hypothesizes that the color vision is because of the different combinations of information of those opposing channels (Hurvich and Jameson, 1957).

To compare these two theories (see Figure 2.2), the trichromatic theory assumes that color vision originates at the receptor level and transmits ratio information to the brain. The opponent process theory holds the idea that the color vision occurs at the neural level, where the brain receives the difference information from the responding cone pairs. These two theories do not stand side by side in isolation since the opponent responding can be produced by three receptors, and both of them are necessary to fully describe the intricacies of human color vision at different levels.

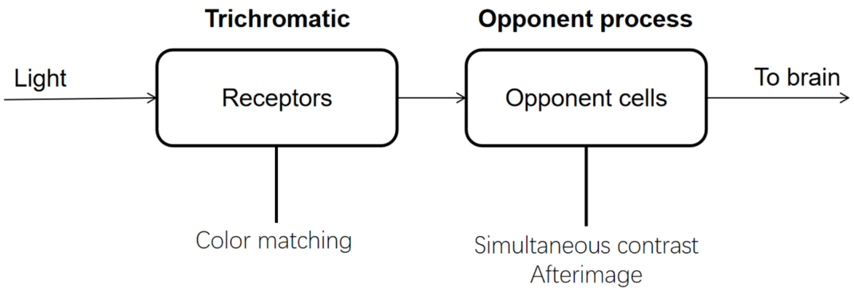

Figure 2.2: *Color vision pipeline*

2.1.3 Perceptual Dimensions of Color

Human's color vision can distinguish different colors by their tone, colorfulness, and shade. Color appearance can be obtained through three perceptual dimensions: hue, saturation and brightness (Figure 2.3).

Hue corresponds to the color naming label, like green, orange, etc. Hue or hue angle refers to radians and determines the position of a color on the color wheel. To convert it into a physical concept, it relates to the dominant wavelength of the color.

Saturation is also called "chroma", describes the colorfulness or the purity of a color. The higher the saturation, the more vivid the color, and vice versa. A saturation of 0% means that there is only monochrome component left.

Brightness refers to the amount of light the color reflected - bright or dark. Brightness axis is perpendicular to the hue-saturation circle, and sometimes it is also called "value".

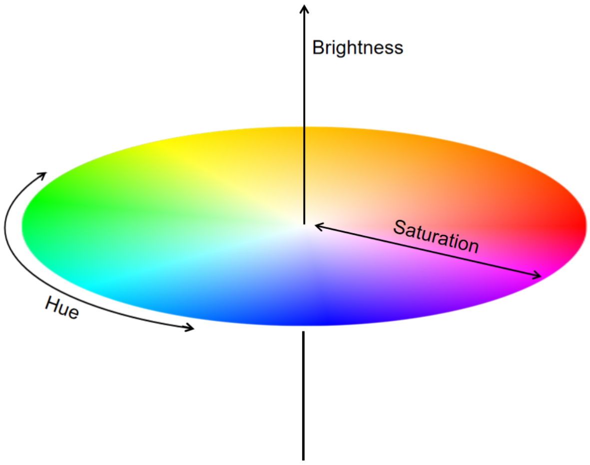

Figure 2.3: *Hue, saturation, and brightness*

2.2 Low Vision

2.2.1 Definition

A functional vision depends on both of the optical and neural factor (Millodot, 2014). In International Classification of Diseases 11th Revision (ICD-11), the diseases related to eyes (and adnexa), the vision neural pathway, and brain area which control visual perception are all in the category of "diseases of the visual system" (WHO, 2018). According to ICD-11, the VA worse than 3/60 defined as "blindness", yet there is no universal definition of low vision. In many papers and professional studies, the "low vision" describes the vision that is not totally blind but has impairment to a certain extent (Corn and Erin, 2010; Leat et al., 1999), which the VA between 6/18 to 3/60 are called "low vision" and the "visual impairment" is for VA between 6/12 to 3/60 (Figure 2.4). In this report, the terms "low vision" and "visual impairment" are all refer to the above definition.

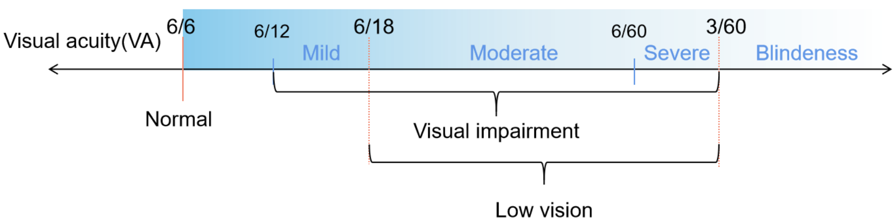

Figure 2.4: *Visual acuity range*

2.2.2 Low Vision in the World

Presently, there are at least 2.2 billion people worldwide suffering from visual impairment, with older adults making up the majority of those with low vision (WHO, 2021). And this number is predicted to continue to rise as the population structure changes significantly in the coming decades (WPP, 2019). Since many visual disorders increase sharply with age (Figure 2.5), including cataract, glaucoma, macular degeneration, diabetic retinopathy, and uncorrected refractive error, the aging trend of the world population would have serious ramifications, though the age-standardised prevalence of blindness and severe visual impairment has declined in recent decades (Bourne et al., 2021).

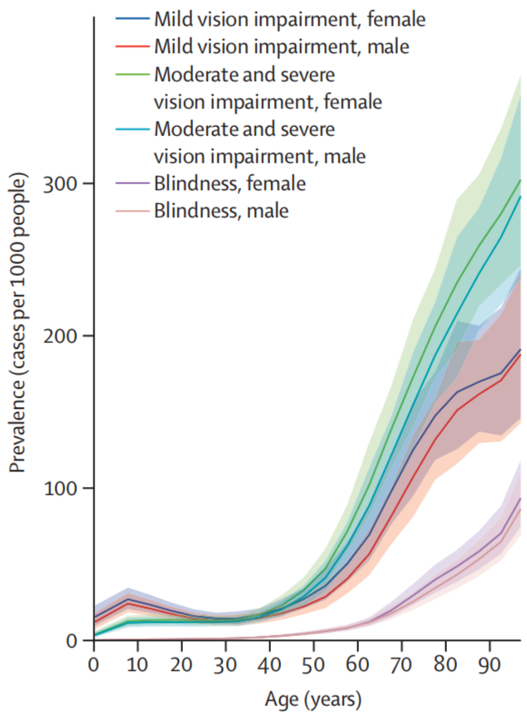

Figure 2.5: *Prevalence of vision impairment in 2020 (Bourne et al., 2021)*

The predictable aging tendency and the enormous group of low vision people in the world not only pose a huge financial burden for the entire society, but also affect the lives of individuals. In addition to the physical limitations that affect their daily activity and productivity, psychological problems, social isolation, and reduced participation in society also have an impact, which can severely affect the quality of life (Stelmack, 2001; Scott et al., 1999; van Nispen et al., 2020; Sawyer and Kaup, 2014).

2.2.3 Some Typical Types of Low Vision

This section briefly introduces the four most common eye diseases, as well as their symptoms and possible treatments.

Presbyopia is the leading cause of near vision impairment, affecting 826 million people worldwide (WHO, 2021). Also, presbyopia is an age-related eye degeneration that becomes noticeable after the age of 40 and worsens after 65. The main symptom is blurred vision at normal reading distance, but can have clearer vision moving the reading material further (Clinic, 2009). This reading difficulty can be corrected with proper glasses or contact lenses.

Cataract is a turbid clouding of the lens of the eye that can make vision foggy and faded. Cataract is also a degeneration of vision that is highly related to the aging process and, in recent years, has become the most common cause of blindness in the elderly group worldwide (Steinmetz et al., 2021). Patients with severe symptoms need surgery, but this surgery is not readily available in many countries (Rao et al., 2011).

Glaucoma is a group of eye conditions with damaged optic nerves, usually caused by abnormally high intraocular pressure. Glaucoma is inherited in families and is more common in older adults. Symptoms vary depending on the type of glaucoma. In chronic open-angle glaucoma, symptoms include severe eye pain, eye redness, and blurred vision, and these symptoms appear gradually and very slowly. In acute angle closure glaucoma, symptoms often include loss of peripheral or central vision. The damage of glaucoma cannot be reversed, but eye drops and oral medications can help lower eye pressure (Lee and Higginbotham, 2005).

Age-related Macular Degeneration (AMD) is a progressive eye disease that mainly affects central vision. It usually first appears at the age of around 50. In the early and intermediate stages, patients may notice misalignment and blurring in the central field of vision. As the disease worsens, the central distortion becomes greater or even a blank space develops in the central field of vision (Jager et al., 2008). There are two types of AMD: wet AMD and dry AMD . The former requires regular eye injections (Lim et al., 2012), but there is no effective remedy currently for the latter. And since most patients have the second type, they need to look for other vision aids to reduce the impact on their lives.

2.2.4 Low Vision Simulation

Currently, there is no way to obtain the vision from others. But there are some simulation techniques in the following that enable normally sighted individuals to get an understanding of visual impairment. However, none of them can simulate the actual sensation of impaired vision.

Image processing method does not affect the view of the viewer itself, but instead changes the objects of observation. For example, Gaussian kernel filters can be used to simulate a blurred view (Lane et al., 2019). And some hazy points can be generated by the computer to simulate scotomas (kumar Krishnan et al., 2019). This end-result way can eliminate the individual difference, and it benefits from its flexibility and low cost, yet it has the disadvantage of very limited mobility.

Goggles are commonly used in many low vision experiments (Copolillo et al., 2017; Zagar and Baggarly, 2010). By using this method, most daily activities can be simulated. However, it still has some drawbacks due to its rigid design. For example, when simulating the AMD, the scotoma on the glasses cannot move with the eye movement, but for the real patients, these distortions or dots always follow their eye movement.

Head Mounted Device (HMD) is a more advanced way to solve the problems of simulation with goggles (Macnamara et al., 2021). With the Virtual Reality (VR) or Augmented Reality (AR) HMD which integrates the eye-tracking technology (Wu et al., 2018), allows users to mimic the vision of various visual impairments. But this more flexible method requires both hardware and software support. Additionally, the users need time to learn and adapt to using the devices.

Contact lenses can also solve the problem of gaze tracking in some specific simulation cases (Almutleb and Hassan, 2020). It is a very mobile-friendly method as the lenses are placed directly on the eyeballs. The main shortcoming is that, as an invasive method, the acceptance of participants is relatively low. And because it is a disposable product, the potential cost is high, especially if it is customized. Additionally, the hygiene issue and eye irritation must also be considered.

2.2.5 Lighting Requirement of Low Vision People

Due to the different eye conditions of people with normal vision and people with visual impairment, they have different preferences for lighting, so the lighting requirements are also different. However, lighting preference is a very subjective assessment. Even with the same eye disease, such as AMD, patients have preferences differently (Haymes and Lee, 2006). Research also shows that there is large individual variation in people's lighting preference (Evans et al., 2010). And there are many factors that influence observer preferences, even the cultural background of the observer plays a role (Park and Farr, 2007).

Nevertheless, there are still some practical recommendations and standards that are suitable for people with low vision and the elderly, since many visual deficiencies start to affect senior people. The primary factor is illuminance. Aging eyes tend to require more light to perceive visual information and become less sensitive to the change of light level (Gordon, 2015). The standard ISO 13586:2000E (2002) recommends that people with impaired vision and older adults should choose a higher lighting level indoors, and gives recommendations on the reflectance of the ceiling, walls, and floor. The Illuminating Engineering Society of North America also provides recommended illuminance levels for various indoor areas for three age groups. Those over 65 age group require much higher illuminance than those under 25 (Hegde and Rhodes, 2010).

Another important characteristic is the Correlated Color Temperature (CCT) value. Elderly people tend to choose the the higher temperature lighting due to their yellowing lenses (CIE, 2017). In addition, the low CCT could negatively affect the Non-Image Forming (NIF) effect (Sinoo et al., 2011). Illuminance and the CCT are combined factors for lighting preference, with preferred CCT increasing with higher illuminance according to the Kruithof curve (Kruithof, 1941). And these two factors not only influence the visual performance, but also have non-visual effects, especial the illuminance (Górnicka, 2008).

Discomfort glare should also be limited for people with low vision, as it can cause the eyes to be unable to adapt to high brightness. The Unified Glare Rating (UGR) determines the degree of glare in a given environment. CIE 190:2010 (2010) gives detailed lighting recommendations for aged people.

There are also many other factors that can influence the observer's vision, such as the lighting type (*e.g.* LED, incandescent), shape, direction, and the luminous distance and spatial perceptions of the luminaires (Butler et al., 2019). A well-designed, high-quality, accessible lighting can enhance the visual performance and well-being of people with low vision.

2.3 Lighting Property

Lighting property is a very comprehensive concept. It not only includes measurable values, but also includes other psychological and perceptual indices. At the present day, there are many evaluation methods and indices to describe lighting properties and quality from different aspects(Kruisselbrink et al., 2018).

In order to elaborate on the lighting physical properties of illumination, two main parts must be considered in this report. One is the physical property of the light itself, which can describe the objective characteristics of lighting. These figures are neither good nor bad, but only show the features of lighting. The other is related to color rendition, since the experiments are based on color discrimination under different lighting conditions. In general, the values of the different metrics reflect the performance of color rendering for the particular light and can serve as an exclusion criterion for light selection. So in this section, only the most relevant indicators of the physical property and color rendering are listed, and some of the other properties are also mentioned in the final.

2.3.1 Physical Property

- Color of Lighting

  CIE x,y value refers to a pair of position in Cartesian coordinate system (figure 2.6) and derived from CIE XYZ system, which is a color system reflects all the colors that human vision can physiologically perceived and its connection with the distributions of wavelengths in visible spectra. And the CIE x,y is the principal value indicates the color of a lighting.

  Correlated Color Temperature (CCT) is a value that approximates the light source's chromaticity coordinates to the blackbody locus. CCT helps to extend the concept of "color temperature" especially for the non-Planckian lighting, using a single number to describe the color tone. Figure 2.6 also shows the Planckian locus of various temperatures.

- Brightness

  Luminous flux is the amount of visible light emitted by a light source with the unit "lumen"(lm) in International System of Units (SI). However, this value does not describe the amount fall on the surface and received by human eyes.

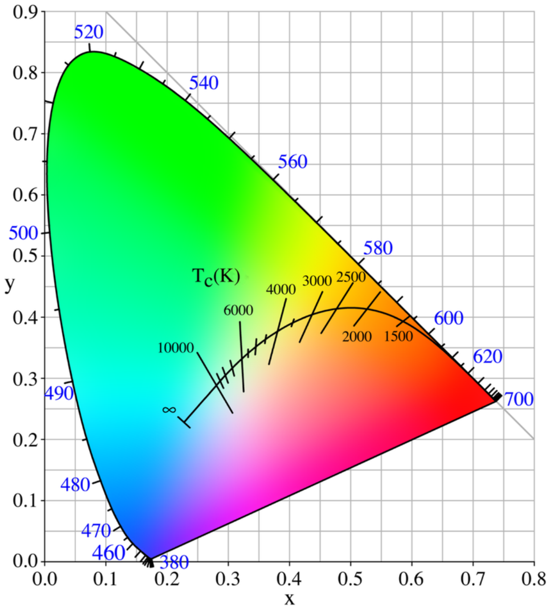

Figure 2.6: *CIE x,y chromaticity diagram*

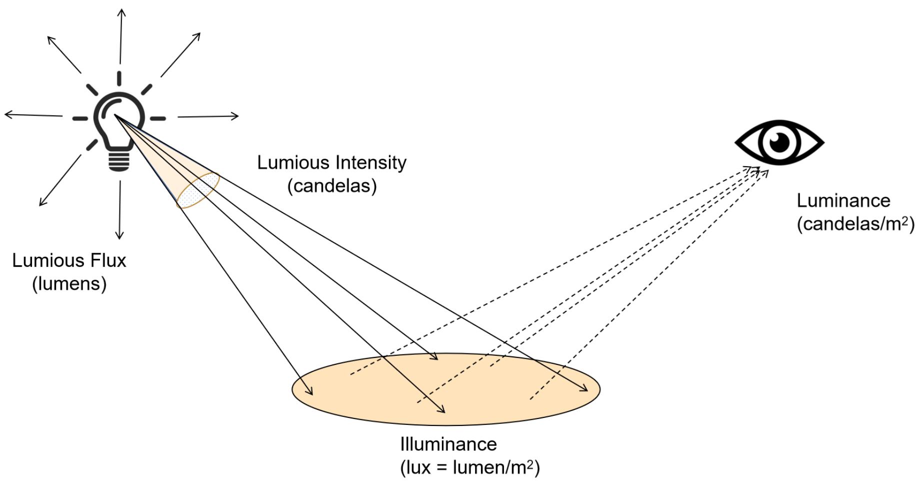

Figure 2.7: *Lumious flux, lumious intensity, luminance, and illuminance*

Luminous intensity is the quantity of light that travels in certain directions from the point light source per unit solid angle. Its unit - "candela"(cd) is one of the base unit in SI.

Illuminance describes the amount of light incident on a surface. The unit lux (lx)(also lm/m^2), which is quantify this amount of light on specific surfaces and objects. It is independent of surface and the direction of the light source.

Luminance refers to the measurement of the amount of light emitting or reflected from a surface and also indicates how much luminous intensity can be perceived by the human eye. The unit for luminance is candela/square meter (cd/m^2), this value varies according to the surfaces and the angle of the light sources.

Figure 2.7 visually shows above concepts and their relationships.

- Energy Efficiency for Vision

Luminous efficiency is the ratio of luminous flux to power in SI. Generally, the LED have a higher luminous efficiency compare to the other traditional light source such as the incandescent lights or fluorescent lights.

Luminous efficiency of radiation is quotient of luminous flux and the corresponding radiant flux for a specified photometric condition(IEC 60050-845:1987, 2012).

2.3.2 Color Rendering Metrics

Color Rendering Index (CRI) (expressed as R_a) is an internationally recognized quantitative measure of a light source's ability to faithfully reproduce the colors of various objects compared to a natural or standard light source (CIE, 1987). The standard light source here is the reference illumination with the CCT of the test light source. By comparing the color difference between the reproduced color of eight Color Evaluation Samples (CES) under the test light and the reference light, the CRI value can show how similar the color is under these two illuminations. The higher the CRI value, the more similar the color is under the test light and the reference light. In addition, apart from the overall R_a value, sometimes the score of the red sample - R_9 is also be specified in many works, because many light source, especially the solid state light sources, are lacking in red content. So the rendering performance in red, which is very important in color rendition like skin color, may hidden in the average CRI value. Due to the same reason, the R_9 is also difficult to have a very high score compare to the scores of the other colors.

Color Quality Scale (CQS) is an alternative method to CRI, and it was designed by National Institute of Standards and Technology (NIST) to address some shortcomings of the CRI, since the CRI evaluates only color rendering and ignores the other characteristics of color quality, and the calculation is outdated for some artificial illuminations. The CQS takes color preference and other aspects into account by including the chroma factor. The CES increase to 15 with higher saturation. Additional, CQS has extended the calculation for all light sources, such as LED, which is more commonly used in recent decades (Davis and Ohno, 2010). Also, the result of CQS is ranged from 0 to 100, avoiding the possible negative result in CRI.

TM-30-18 is issued by Illuminating Engineering Society (IES) in 2018, which is an expansion of former standard TM-30-15. As a color rendition standard and reporting format, TM-30-18 is widely used and accepted especially for the solid-state lighting evaluation. The two main average outputs of TM-30-18: color fidelity index and gamut area index are from 99 different CES which are categorized into 16 hue-angle bins. The hue shift and chroma shift of each bin are all have visual presentation in the color vector graphic. The color fidelity index of TM-30-18 also has no negative value and the maximum score is 100, that being an exact match to the reference color. The other value, gamut area index, can exceeds 100, which reflect an increased saturation. Instead, the value under 100 means desaturated some colors.

Color fidelity index (R_f) is a new color rendering metrics published by CIE (CIE 224:2017, 2017). It is not designed to replace the CRI, but to solved some existed problems in CRI. It is driven by some modern methods, standards, and new equipment (Jost et al., 2018). One of the most significant changes is that instead of only using 8 color samples, R_f uses 99 CES which is nearly uniformly distributed in color space. It also changed the working color space from CIE 1964 U*V*W* to CIE CAM02 and the chromatic adaptation to CIE CAT02. Another update is R_f introduces the blended black body and daylight between 4000K to 5000K as the reference light source. As with CQS and TM-30-18, the color fidelity index has the lowest value of 0 to the up boundary 100, which makes the R_f more understandable.

2.3.3 Other Indices

There are also a plenty of other light source indices. For example, the Unified Glare Rating (UGR) (CIE 117-1995, 1995), which evaluating the glare degree in a given environment. And the Gamut Area Index (GAI), which is used to compare the gamut area of a test light source with the gamut area of a reference light source. Apart from these physical features, light also have some other perceptual, psychological and non-visually effects (Bao et al., 2021). Correspondingly, there are also some metrics to quantified these influence. For example, the Circadian Efficacy of Radiation (CER) and Circadian Luminous Efficacy (CLE) are describe how the circadian system perceive the non-visual radiation and how non-visual light is emitted from artificial light sources, especially LED lights (Hye Oh et al., 2014; Oh et al., 2015).

3 | Related works

There are a variety of assistive approaches for the visually impaired. Based on the type of feedback, they can be roughly divided into two parts. One part is the assistance method with non-visual feedback, which means that the necessary information is transformed and provided to the user in a form other than visual, such as sound, vibration, or electrical. These aids mainly help people with severe visual impairments and blindness, as they have little residual vision. Another part is the visual feedback assistant method, which can enhance visual information to help users access it. These techniques are especially helpful to people who still have functioning residual vision. The proposed method also belongs to this type.

3.1 Non-Visual-Feedback Assistance

Users with serious eye conditions need additional cues to obstacles or object information in daily life. In the early age, sensor-based devices can help people detect the distance of obstacles, helping them avoid potential obstacles. With faster digital imaging technology, camera-based aids are being introduced to provide more accurate information.

3.1.1 Sensor-Based Smart Cane

Canes are commonly used among the visually impaired people as a primary mobility aid tool, and are especially useful outdoors. The traditional cane can help low vision people detect obstacles on the sidewalk and ground irregularities. However, it is limited when the potential collisions are on the user's side or above the user's waistline.

Various electronics-embedded smart canes have been launched to avoid these limitations. Most Electronic Travel Aid (ETA) use different sensors, such as ultrasonic sensors and infrared sensors, to determine distance to improve spatial perception(Islam et al., 2019). Some handheld devices retain the shape of a cane that integrates the controller, micromotor, battery, and sensors (García et al., 2011; Bhatlawande et al., 2014; Ito et al., 2005; O'Brien et al., 2014). And some modified canes have more functions by adding external components such as wheels and tactile indicators (Jeong and Yu, 2016; Shoval et al., 2003; Salat and Habib, 2019). However, the large size and limited detect area may cause inconvenience when used in real life (Ulrich and Borenstein, 2001).

Also, most of the above ETA approaches have a major drawback: apart from the distance of the obstacle, they cannot provide the size, movement status and other information (Hossain et al., 2011). And those devices requires users to scan the walkway continuously to find the path.

3.1.2 Camera-Based Assistant Devices

With the high speed development of image processing and computer technology, the camera has the ability to be introduced into the ETA devices to provide more information of obstacles. These auxiliary systems usually consist of one or more digital camera systems, a computing and processing unit, and a feedback unit (Islam et al., 2019). The feedback could be vibration (Aladren et al., 2014; Zelek et al., 1999), electro-tactile (Meers and Ward, 2005) or acoustic information, including the audio signal (Meijer, 1992; Aguerrevere et al., 2004; Yang et al., 2016; Söveny et al., 2014; Bai et al., 2017) and stereo sound (Kang et al., 2017; Yang et al., 2018). Some systems can also perform classification or recognition based on the captured image information and provide various feedback to the user. (Aladren et al., 2014; Mekhalfi et al., 2016). In addition, some system with incorporated Global Positioning System (GPS) can obtain landmarks for better obstacle avoidance and navigation function (Meers and Ward, 2010; Kammoun et al., 2012; Dakopoulos and Bourbakis, 2008).

3.2 Visual Feedback Assistance

For the people with less severe vision impairment, they still able to leverage their functional vision to access visual information. Corrective lenses (including eyeglasses and contact lenses) for myopia and hyperopia are the most typical and widely used aids of this type. The following methods provide different vision enhancement techniques to enable users with other visual impairments to achieve better vision.

3.2.1 AR Glasses

The Augmented Reality (AR) is a subset of Mixed Reality (MR) which connect between the real environment and the virtual world (Milgram and Kishino, 1994). With the AR head-mounted set, users can see the virtual object integrated with the real world. Because of the real-time interaction characteristic of AR (Azuma et al., 2001), there is an opportunity to utilize the AR headset to assist the visually impaired (Carmigniani et al., 2011). There are various ways to enhance the vision for the HMD, for example, magnification (Stearns et al., 2017, 2018), edge enhancement(Hwang and Peli, 2014), contrast enhancement(Ehrlich et al., 2017), or combine many functions with brightness adjustment, color enhancement (Gopalakrishnan et al., 2020; Zhao et al., 2015).

Most of the research above benefit the low vision people in terms of increasing the visual performance. But there are still some shortcomings:

- Unlike the human eye, which can control the thickness of its own lens by controlling the stretching and contraction of the ciliary muscle, and then adjusting the focal length, the AR system can only help either near or distance vision (Gopalakrishnan et al., 2017).

- Users need to spend time learning and adjusting how to use these devices. It is also important to notice that older adults make up a large portion of the visually impaired population (WHO, 2021). Thus, we need to consider the difficulties and motivation of older people to learn how to use a new digital device (Ringering and Amaral, 2000). The research of Culham et al. (2004) concluded that older patients would be less likely to benefit from HMD because of the relatively low familiarity with technology. In addition, adaptability is one of the most important considerations when evaluating a device (Findlater and McGrenere, 2004), Since most HMDs are relatively heavy, this may decrease users' willingness to use them (Rolland and Hua, 2005).

- Although some studies use commercial HMDs that are already on the market (Hwang and Peli, 2014; Stearns et al., 2018, 2017), they are still not affordable for many people (Huang et al., 2019; Sandnes and Eika, 2017). The lower use of these HMDs would indirectly affect social acceptance (Lorenzini and Wittich, 2020).

3.2.2 Lighting Assistant

Unlike a wearable device like HMD, a less bulky method is to use custom lighting. It is necessary to customize the lighting system because the preferred lighting of the visually impaired people differs from that of the normally sighted (Rotruck et al., 2015).

Many recent researches has demonstrated that the illuminance and the color temperature can affect the visual performance of low vision people (Evans et al., 2010; Wittich et al., 2018; Henry et al., 2020), and the quality of life of them can be improved by improving lighting conditions (Brunnström et al., 2004; Turid Borgestrand, 2021). Apart from these two factors, there are some other features or methods of lighting system are investigated to facilitate vision rehabilitation.

Sa-Ngadsup et al. (2018) proposed a lighting edge enhancement method for independent navigation of visually impaired people. A psychophysical experiment on autonomous mobility was conducted. Three distinct types of visual impairments were considered in the experiment. The result shows that the proposed lighting system has the potential to benefit the people who suffering from tunnel vision and central scotoma. But the effect for the blurred vision people are still uncertain.

A recent work of Katemake et al. (2019) involves three sub-experiments. Apart from the illuminance level & CCT and edge enhancement, the third experiment - color contrast enhancement - found that manipulating the light spectrum to increase color contrast can satisfactorily improve mobility in cataract patients. This result allows us to hypothesize that adjusting the Spectrum Power Distribution (SPD) could be an approach to facilitate people with visual impairments to improve their daily mobility, especially under the indoor environment.

4 | Methodology

Color is one of the key factors for HVS to detect and identify objects. The greater the color difference, the greater the likelihood that both normally sighted and visually impaired people will be able to differentiate the objects. Technically, the color difference can be changed by using different lights, or more precisely, different spectra. The tunable multiple channel LED light has the advantage of being able to flexibly adjust the spectrum by varying the intensity of the individual channels. A set of experiments targeting a specific type of visual impairment - central loss vision - was devised, which is the main symptom of AMD. A 24-channel LED lighting system was used to optimize the mixed light spectrum and increase color contrast to improve the visual performance of people with visual impairment in terms of color discrimination.

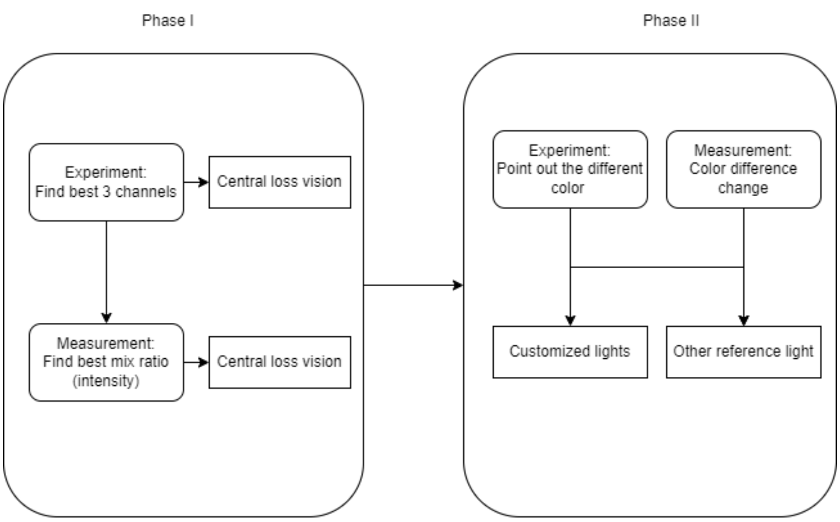

Figure 4.1: *Experiment flowchart*

The proposed experiment consists of two phases designed to address two continuous questions: "What is the ideal LED light combination for color discrimination?"

and "How well does the optimized light allow for color differentiation?" Since Phase II experiment can also viewed as a validation of Phase I experiment, to make this chapter less tedious, the Phase II is located under Chapter 5 "Result Validation". Figure 4.1 depicts the general flowchart for the set of studies.

In this chapter, there are two primary procedures in order to acquire the ideal LED mixture: selecting the channels and adjusting the intensity, which correspond to the two primary parameters for generating a spectrum with an LED lighting system.

4.1 Determination of Channels

Due to LED's high luminous efficiency, high energy efficiency, and extended lifespan, it is becoming increasingly popular around the world. Because this optimized light needs to be used for low vision people as a daily-use illuminator, the final light expected from this study should be white or close to white.

There are two basic methods for manufacturing white light-emitting diodes. One approach is to employ phosphor material to transform monochromatic light from a blue or ultraviolet LED into white light with a broad spectrum, akin to a fluorescent bulb. Alternatively, white light can be generated by combining a number of separate LEDs. Due to the feature of LED itself, it requires at least more than two wavelengths to generate the white light based on color mixing technique to approximate the black-body radiation (Pimputkar et al., 2009).

On the market, multi-channels white LEDs are often composed of red, green, and blue, and they offer the option to mix different hues. It is also the result of marketing selection that strike a balance between cost, color rendering, and luminous efficiency. However, there is no standard market specification for the peak wavelength, Full Width at Half Maximum (FWHM), etc. of the three channels of lights. Therefore, it is still keep three channels in the proposed experiment, and the goal is to identify three new channels that can improve the color discrimination performance of individuals with specific visual impairments.

4.1.1 Apparatus, Materials and Experiment Setting

The lighting system that used in this experiment is the first 24-channels LED lighting system (Telelumen, United States) in the Europe. It includes both visible and invisible channels, ranging from Ultraviolet (UV) to Infrared (IR). Figure 4.2 illustrates the SPD for every channel.

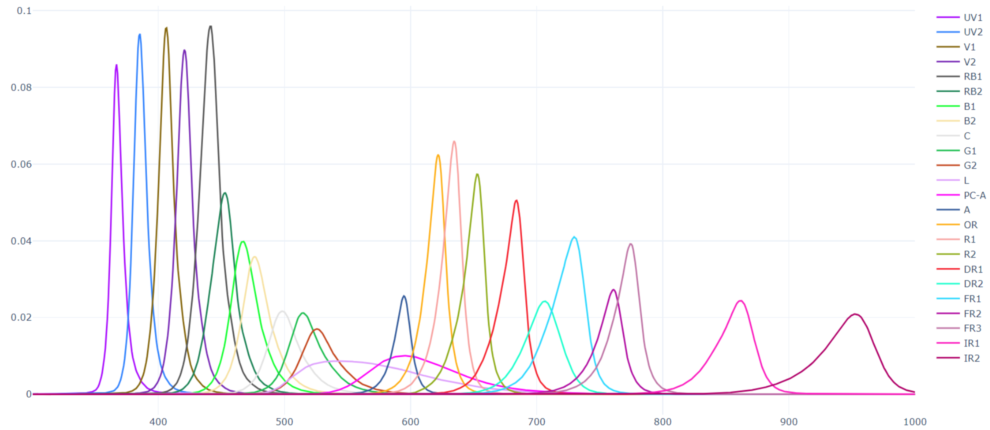

Figure 4.2: *SPD of 24 channels LED lighting system*

However, not all channels are appropriate for the experiment. Figure 4.3 depicts a series of criteria selection criteria for channels. Since the UV radiation may provide a fluorescent effect and harmful for human eyes if overexposed, it has even been linked to some ocular diseases (Yam and Kwok, 2014). Consequently, the UV component should not be considered in the design of interior illumination. In addition, there are two light channels whose power is predominantly concentrated on wavelengths longer than 800 nm, which are invisible to the human eye. Therefore, these two IR lights need to be removed.

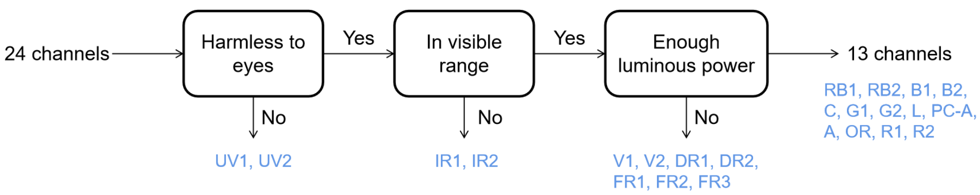

Figure 4.3: *Flowchart of channels selection*

Apart from the aforementioned requirements, the brightness of the light is also essential. The formula (4.1) below can be used to compute the required total light output Φ_l, where W and L are the width and length of the area that need to be illuminated. Figure 4.4 shows geometry of observation. The main observation area is a 45 cm diameter circle, but the majority of the experiment activity is in all the central area of the table, hence W and L represent the table's width and length. And in this case, the lighting level is set as 50 based on the footcandle lighting index recommended by IES. Additionally, various other elements, such as wall color and light placement, can impact the needed light output, so the final Φ_l need to be fine-tuned according to the actual situation. According to the geometry of the experiment setting and the type of application, the final minimum required light output in the experiment space is 280 lumen. This value has also been visually evaluated by many observers to ensure that it adequately illuminates the task area and is neither too dim nor too bright for the eyes.

$$\Phi_l = W \times L \times lighting\ level \tag{4.1}$$

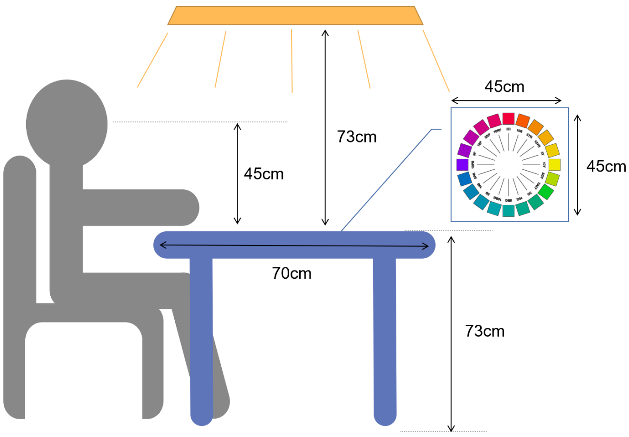

Figure 4.4: *Experiment setting*

Based on the required output power, thirteen channels are sufficient for the following psychophysical experiment, and each available single channel is set to the same illumination level. To examine the more detailed information of each channel's maximum luminous flux, peak wavelength, and FWHM, see the Table A.1 in the appendix.

Besides, the experiment was conducted in a dark room with black walls, black floor, and furnished with neutral grey table. There were two windows with black opaque curtains blocking the light from outside to ensure that only the experimental LED light was used for the observation. When there are no indoor artificial lights, the illuminance of this dark room is under 1 lux.

4.1.2 Participants and Experiment Design

The primary procedure of this psychophysical experiment is to propose a test of color arrangement using all of the selected different channels of light one by one. After obtaining the arrangement results from the observers, select three channels that are capable of producing white light and have a maximum "color discrimination range" from the results of the experimentation with observers.

16 observers (5 females, 11 males) of 10 nationalities and ages ranging from 22 to 42 participated in this psychophysical experiment. Before the proposed experiment, all of them resulted in "No Colorblindness" on the D-15 Color Arrangement Test. And all of them have normal or corrected-to-normal VA.

Before the experiment began, each participant was assigned a central scotoma simulation goggle (Fork in the Road, United States) with an VA of 6/60 and had 1-2 minutes to adjust. All the volunteers need to wear these goggles for the duration of the experiment.

The observers are then instructed to perform the color arrangement task under each channel of light. Figure 4.5 shows the arrangement task of 20 selected color samples from Munsell color system with the identical chroma value 6 and value 6 but different hues. These color samples are all 3×3 cm square with matt finish. Among these 20 hues, five primary hues (5R, 5Y, 5G, 5B, 5P) are used as reference samples which in the fixed positions (shown as the black dots in the Figure 4.5), and the observers need to arrange the other 15 samples based on the positions of these 5 reference samples. In addition, little dot markers were placed on the table to remind participants where to place the color samples. Observers are also informed that the reference color samples cannot be moved, that they must use all the of the other color samples, and that there must be three samples between each pair of reference samples. Figure 4.6 includes two photos of this psychophysical experiment.

There was no time limit for the task, but observers would receive a reminder if they spent more than eight minutes in an arrangement. After the observer completed the arrangement, the same lighting system would switch to a 6500K daylight setting. Additionally, to more efficiently record results, each sample is encoded with a number from 1 to 20 clockwise from 10R 6/6 (These numbers are represented in Figure 4.5 as the numbers in the corners of each color sample), and the final arrangement order was recorded as the order of these sample numbers. These numbers are on the back of the samples, thus experiment viewers were unable to see them during the experiment.

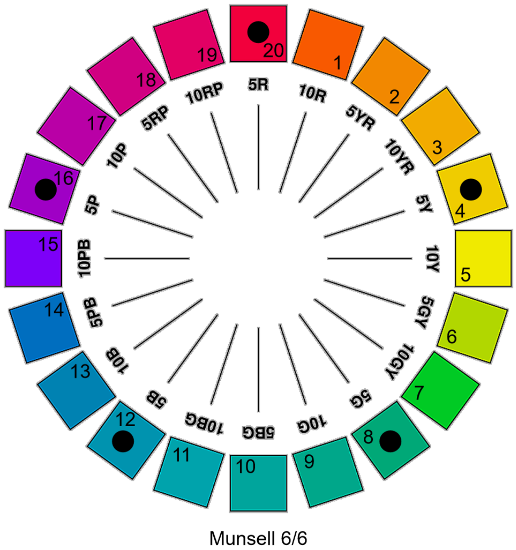

Figure 4.5: *20 hues in Munsell color system (value 6/chroma 6)*

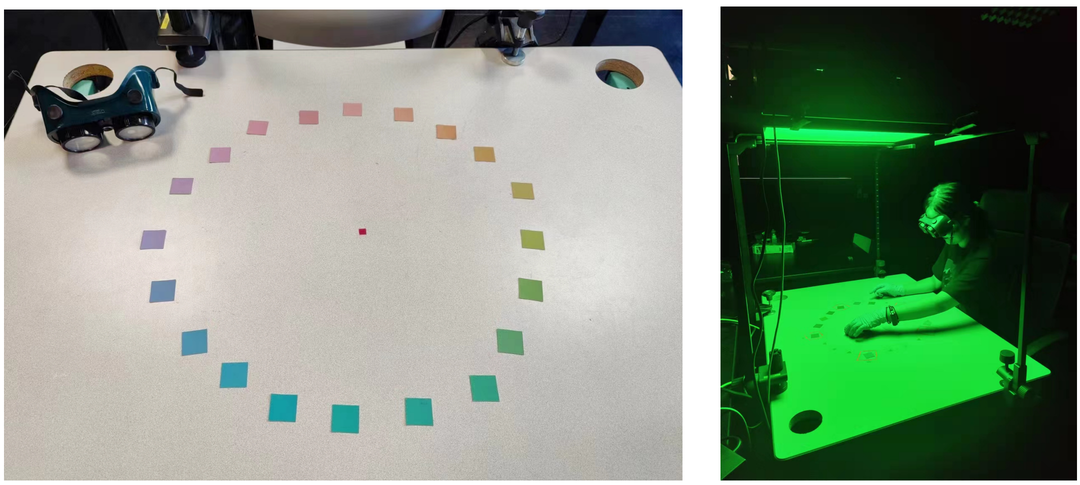

Figure 4.6: *Photos of experiment*

Since there are 13 channels of light are chosen, the arrangement need to be repeated 13 times in total for each participate. Considering that lengthy trials would affect the reliability of the results and cause fatigue to the subjects, the experiment was split into two sessions of approximately 45 minutes each. The configuration of each experiment remained the same.

4.1.3 Data Acquisition and Analysis

The outcome of this arrangement test employed the similar scoring method as the Farnsworth-Munsell 100-Hue Test (Farnsworth, 1943), which calculated by the sum of differences of adjacent numbers. Unlike the Farnsworth-Munsell 100-Hue Test, which uses 100 numbers, the number assigned to each sample in our experiment ranges from 1 to 20.

In this psychophysical experiment, as the observer performed the arrangement under several narrow-band lights, it is very difficult to have all correct results, even if the observer has normal color vision, thence the arrangement results can reflect the properties of light. The greater the error score, the worse the color discrimination; conversely, the lower the error score, the better the color discrimination. The objective in this step is to identify the optimal combination of three lights with low error scores in practically the entire color circle.

In addition, participants have demonstrated individual differences in the performance of the arrangement. Before summing up the result scores of each channel from several observers, the score of each observation is normalized to ensure that each observation has the same weight and to decrease the impact of extreme values. Figure 4.7 shows the results of all the 13 test lights and follows the result plotting rules of the Farnsworth-Munsell 100-Hue Test. The polar coordinates correspond to the circle of color samples in the experiment, and the solid line with dots represents the average score for each channel. The colored sector means the range with relatively low error, indicating that color discrimination is good in that range under the current illumination. The "pass" threshold that determines whether or not the color discrimination is accurate is set to zero, and the "pass range" is defined as the current and neighboring errors that are all below the threshold. Therefore, the "pass range" can indicate the hue range of each channel's good color discrimination.

For example, the channel 5 (RB1) is a blue narrow band light, under this light, it is difficult to discern red and green, but yellow and blue hues can be differentiated easily. So in the Figure 4.7 a), the green (near 135°) and red (near 315°) areas have high result values, but the yellow and blue range are colored due to their low error scores.

With the 13 "pass ranges" (see Figure 4.7), the possible mixture of 3 channels can be generated. By collecting the absolute values of each channel's "pass range" and merging them together, the whole "pass range" of various combinations can be created. Figure 4.8 is an example of the combination of channels 5 (RB1), 8 (B2), and 16(R1). In lieu of using the "pass range" colors, the sector's color is chosen as

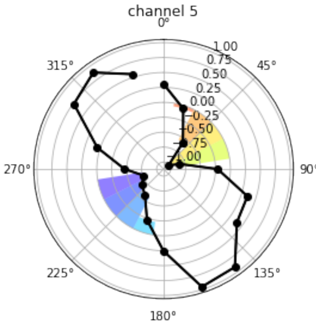

(a) *Channel 5 - RB1*

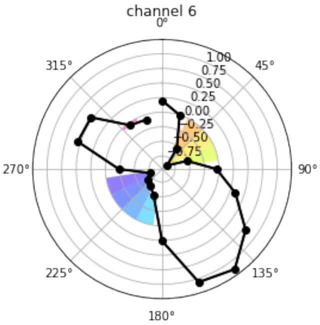

(b) *Channel 6 - RB2*

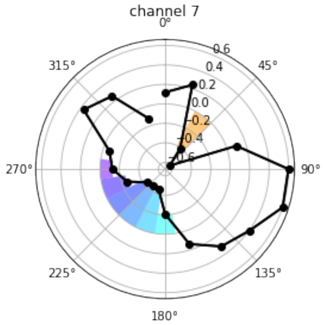

(c) *Channel 7 - B1*

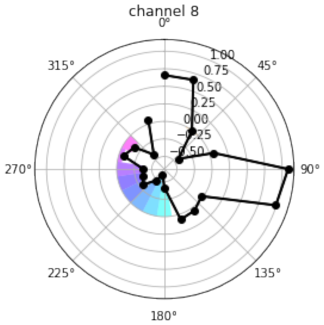

(d) *Channel 8 - B2*

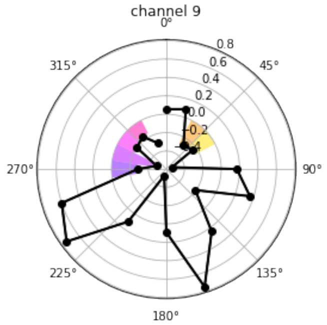

(e) *Channel 9 - C*

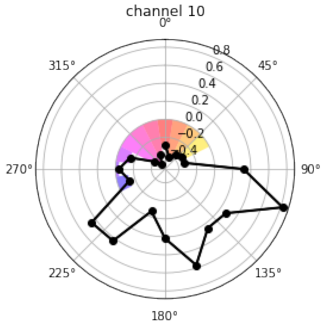

(f) *Channel 10 - G1*

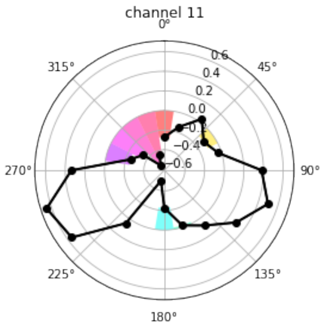

(g) *Channel 11 - G2*

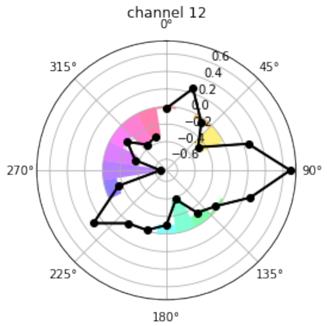

(h) *Channel 12 - L*

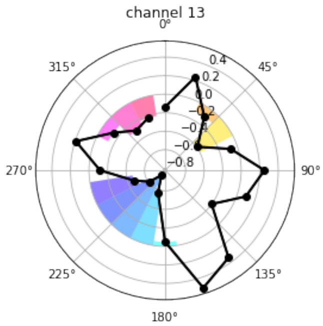

(i) *Channel 13 - PC-A*

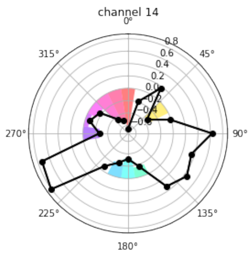

(j) *Channel 14 - A*

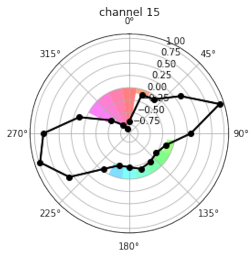

(k) *Channel 15 - OR*

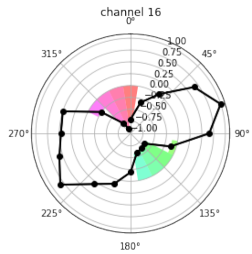

(l) *Channel 16 - R1*

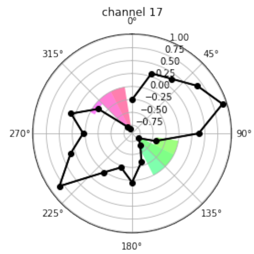

(m) *Channel 17 - R2*

Figure 4.7: *Experiment results of 13 channels*

the color that close to the real lights for a more comprehensible visual effect. And the sector's area reflects the how good of the score because it is inversely connected with the error values. Due to the additive properties of the light, the overall area and shape can represent the current mixture's capacity for color discrimination. Additionally, the overlapped area is computed only once, thus the theoretical maximum area for this experiment is the entire circle, and by calculating the area filled by all the generated shapes in the full circle, an ranking list of different channel combination can be obtained.

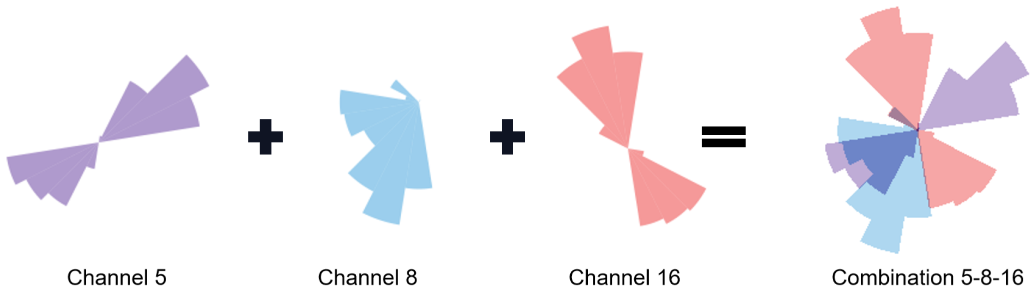

Figure 4.8: *An example of 3 channels combination*

4.1.4 Results

There were 286 distinct possible combinations formed ($_{13}C_3$) in this step. To select the appropriate combination, the mixture with wider range (360 degree all-hue circle ideally) and larger "pass range" might be capable of good color discrimination. Another crucial criterion is that the selected three channels must be able to produce near-white light, or the color of light at the Planckian locus.

Among all the lights, channel 12 (L) and channel 13 (PC-A) are the only two non-narrow channel lights, hence the lights including these two channels are ranked highly since they have a larger "pass range". Also, several different combinations of red-green-blue lights have a good "pass range". In this step, it is difficult to determine which option is the best, and it is worthwhile to explore how performance varies between different combinations. So after screen out through all the possible mixtures, three distinct combinations were chosen. There are 6-10-13, 6-11-16, and 6-12-16. Figure 4.9 shows the result plots of these 3 selected channel combinations. These three combinations would be investigated further in the next steps.

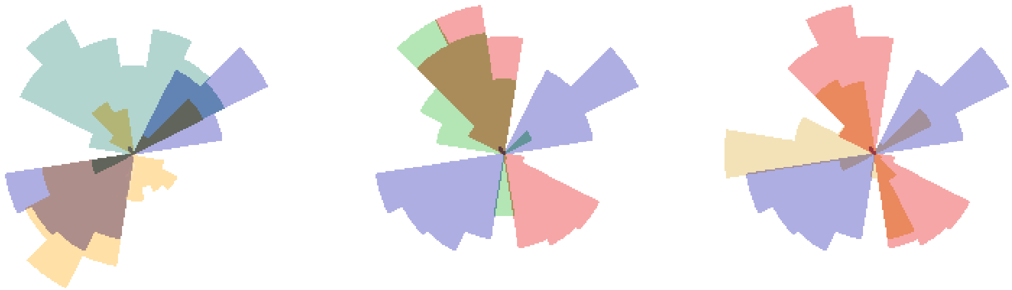

(a) *Channel 6-10-13* (b) *Channel 6-11-16* (c) *Channel 6-12-16*

Figure 4.9: *Channels combination results*

4.2 Determination of Mix Ratio

Following the selection of channels, their intensities need to be determined. The purpose of this section is to determine the ideal ratio between the three selected channels based on their respective measurement results. Several lighting metrics are employed to eliminate insufficient lighting and arrive at the appropriate ratio.

4.2.1 Method

The numerical results of light are beneficial for the further more accurate data assessments. In this mix ratio determination step, many mixing ratios are enumerated using the exhaustive approach, and then the ideal mixing ratio is filtered out based on a large number of measurement results and the scoring procedure.

There are numerous metrics that may be used to evaluate a light source, but in this instance, there are three characteristics that characterize "excellent" light: high color rendering fidelity, a wide color gamut area, and a low Duv. High color fidelity means the lighting can reveal the true color when compared to natural light; high color gamut indicates that the light can make the color more saturated, which can aid to increase color contrast; Low Duv means the light is close to Planckian locus, making it suitable for daily use. However, these three conditions cannot be met simultaneously, hence, it is essential to make trade-offs.

In this step, a large number of lights are generated, necessitating the application of a series of filtering requirements. Figure 4.10 shows the selection procedure of the mixing ratio using light combination 6 (RB2)-11 (G2)-16 (R1) as an example. The entire procedure involves both a coarse and a fine adjustment. Coarse adjustment through the elimination of non-compliant lights to narrow the acceptable intensity range of each channel; fine adjustment is used to find the optimal mix ratio in smaller increments.

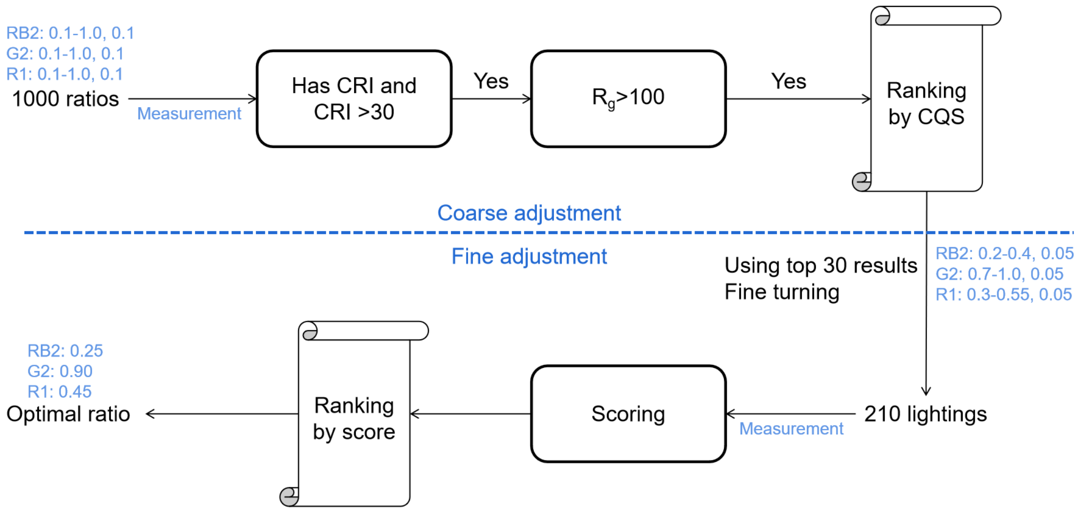

Figure 4.10: *Filtering processing of ratio choice*

Firstly, the intensity of three selected channels is adjusted from 0.1 to 1 in increments of 0.1, which results in $10 \times 10 \times 10 = 1000$ different illuminance. And all the 1000 lights played sequentially, while the spectroradiometer Sectraval 1511 (JETI, Germany) measured the current illumination information, including CRI, CQS, Duv and CIE2017 color fidelity index. In this coarse adjustment stage, the primary objective is to filter out invalid lights; the CRI value is an essential and straightforward indicator of how faithfully the light reproduce color; if the light has no CRI or the CRI value that is too low, it is not suitable for the application. On the basis of the measurement results, the criterion for excluding the lights without CRI values or with a CRI of less than 30 is then used. In addition, the color gamut index (R_g) can reflect the saturation and discrimination more accurately and consistently better predicts performance on the Farnsworth-Munsell 100 Hue test more accurately than CRI (Rea, 2010). Therefore, the lights with color gamut values below 100 are eliminated. After applying these filters, arrange the remaining lights according to their CQS values, as CQS is a comprehensive metric of the light evaluation. This phase of ranking establishes the valid intensity range for each channel. For instance, the intensity range of each of the three channels of light combination 6 (RB2)-11 (G2)-16 (R1) was all reduced by more than 60% in this step.

The intensity value range of each channel can be narrowed down thereafter depending on the top 30 values in the ranking list. With the restricted intensity range, the new increment is set at 0.05 in order to achieve more accurate results. The newly created light set was then measured as in the preceding phase. In this application, there is no universal formula for calculating and scoring the appropriate light, thus we must develop our own scoring mechanism. To avoid mononumerosis, the formula should have a variety of components. As stated previously, the color rendering index, the color gamut area, and the Duv are the three most important parameters in this instance. Formula 4.2 is the scoring method with a weight of 50% for color fidelity, 50% for color gamut area, and a penalty for high Duv. The 50% of color fidelity are from CQS, TM30-18 color fidelity index and the CIE2017 color fidelity index respectively. CRI is not include in this formula because CIE (2007) Technical Report states that when white LED light sources are included in a collection of light sources, CRI is inapplicable for predicting the color rendering rank order of the light sources. Finally, the light with the highest score is selected as having the optimal mixing ratio after all valid lights have been graded according to the customized formula.

$$Score = 0.3 \times Q_a + 0.5 \times R_g + 0.1 \times R_f + 0.1 \times CIE\ 2017\ R_f - 100 \times Duv \quad (4.2)$$

4.2.2 Results

All the three selected channels combinations went through the filtering process. In the following text, $L1$, $L2$ and $L3$ refer specifically these 3 optimized lights respectively. Table 4.1 shows some numerical results of those three lights. For more detailed information and data, please refer to the appendix.

Table 4.1: *Information of 3 generated lights*

Lights	$L1$	$L2$	$L3$
Channels	6-10-13	6-11-16	6-12-16
Intensity	0.3-0.6-0.7	0.25-0.9-0.45	0.225-0.675-0.36 [a]
CCT	6707K	5279K	3077K
Duv	0.0020	-0.0016	-0.0292
CRI	93	42.46	75.1
CQS	92.94	52.36	77.8
TM-30-18 R_f	90	67	80
TM-30-18 R_g	104	127	121
CIE color fidelity index R_f	90.4	66.6	80.5

[a] Normalized intensity to converted to the same illuminance as $L1$ and $L2$

Figure 4.11 includes the spectrum of each lights, and the figure 4.12 is the TM-30-18 Color Vector Graphics (CVG) of these three lights, which shows how each hue bin shift. These figures illustrate the similarities and difference between these three output lights.

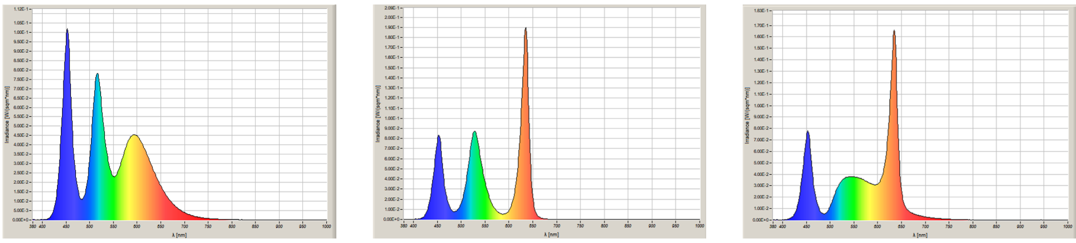

(a) $L1$ (b) $L2$ (c) $L3$

Figure 4.11: *Spectra of three output lights*

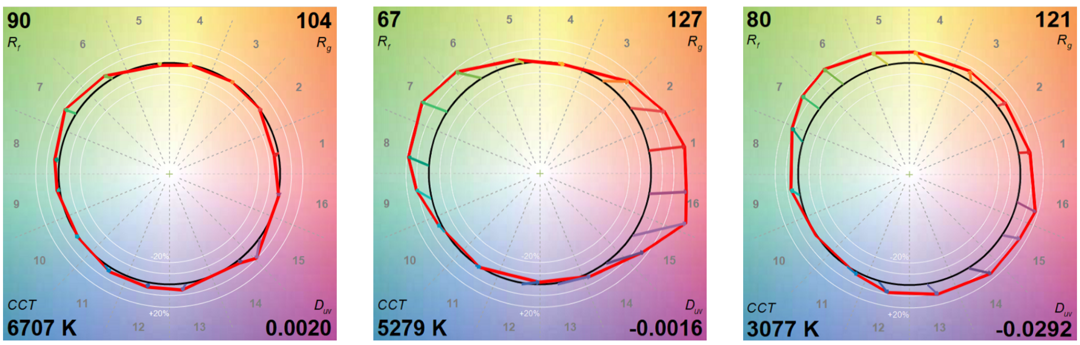

(a) $L1$ (b) $L2$ (c) $L3$

Figure 4.12: *TM-30-18 color vector graphic of three output lights*

Also, it is worth noting that each of the three lights meet two of the three criteria: high color rendering index, high color gamut area, and low Duv. Figure 4.13 visually depicts the characteristics of these three lights. In the TM-30-18 R_f & R_g, the three red dots represent the positions of $L1$, $L2$ and $L3$. The white and light grey regions (area ① and area ②) represent the boundaries of the light source on the Planckian locus and the limitations of the practical light source, respectively. $L1$ has high fidelity index and low Duv, it located in the middle-right portion of the graph and in the area ①. $L2$ has high gamut index and low Duv, it also within the area ① but near the boundary between area ① and area ②. The $L3$ has relatively high color gamut index and fidelity index, but also a high Duv, in the diagram, it lies towards the edge of the practical light restrictions on the shown graph.

After obtained these customized lights, they need to be further validated and tested by experiments in order to evaluate their color discrimination performance. In addition, it is intriguing to observe how the outcome will vary under these various lighting conditions.

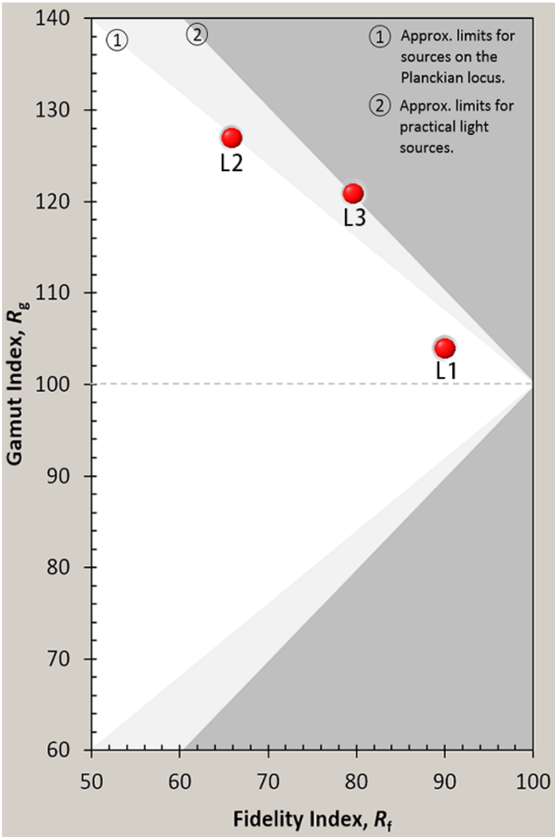

Figure 4.13: *TM-30-18 R_f & R_g of three output lights*

5 | Result Validation

In this chapter, the optimized three lights are validated by psychophysical experiments and color difference measurements to determine if they can enhance the color discrimination in order to aid patients with central scotoma. This is also the Phase II experiment of the procedure (entire workflow see Figure 4.1).

5.1 Experiment

The purpose of this experiment is to validate the customized illumination spectrum in terms of color discrimination. Due to the fact that people with central loss of vision do not have a complete visual field, it is difficult for them to differentiate between a large number of objects. On the basis of this property, a psychophysical experiment is devised to examine the performance under various lighting situations.

5.1.1 Materials and Experiment Setting

In this experiment, four distinct spectrum of light were utilized. In addition to the $L1$,$L2$ and $L3$, another white LED system (CCS LFL-360-SW, Japan) were used as the reference. This lighting system is a rectangular LED panel that emits white light that is uniformly distributed. Also, with its adjustable power supply, its illuminance can be controlled to the same as others lights. This is a phosphor-converted white LED light that is also commonly used for indoor lighting. In the subsequent article, LW refers specifically to the white LED that utilized in the experiment.

The psychophysical experiment was conducted in the same place as the previous Phase I experiment. All the configuration and observation geometry remain unchanged. Besides, the illuminance of all the lights is 500lx, which is the recommended illuminance for classrooms and offices in the task area according to the European Commission's Premium Light Pro project(Kofod, 2017).

5.1.2 Participants and Experiment Design

This experiment involved 15 participants (11 males and 4 females) from 10 different nationalities with the average age of 24 ± 3 years old, all of whom had normal or corrected to normal VA and have no color blindness. Also, the observers need to wear the central scotoma simulation goggles (Fork in the Road, United States) with VA of 6/60 during all the experiment.

The test color panels are composed of Natural Color System (NCS) samples. Figure 5.1 depicts the panel's design specifications. The experiment panel is a 260 × 260 mm square with neutral grey frame. On each color panel, the color patches are organized in a 5 × 5 grid with a 30 × 30 mm grid size. There are 24 samples in each panel, 23 of which are reference samples and 1 test sample (no sample in the center). The color of the test sample differs from that of the reference sample, but they are otherwise very similar. In Figure 5.1, the test color sample is marked with blue hexagonal star. Also, to make the experiment has sufficient difficulty, the color difference between the reference sample and the test sample should not be too large or too small. Delta E 2000 (or dE 2000) is the most precise CIE color difference method currently available. The range of dE 2000 values between 1.5 and 3.5 is appropriate for this application.

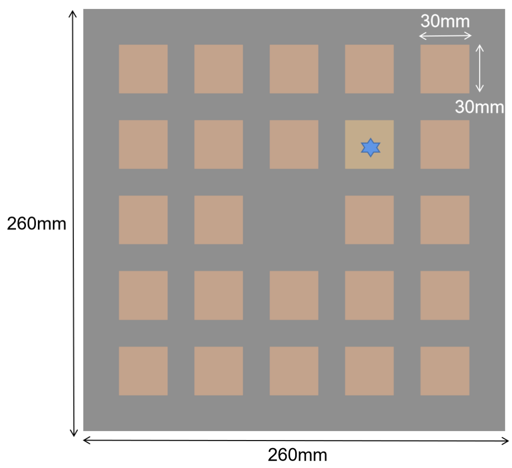

Figure 5.1: *Experiment panel design*

Eight different panels are used in the experiment. Figure 5.2 indicates the sample selection of these 8 panels. The reference colors are the four primary colors and four inter-colors of the NCS, and the test colors are chosen based on hue proximity to the reference colors. But B50G is an exception since the color difference between nearby colors and the reference is insufficient to distinguish them. In particular, the reference color and test color have the same saturation and blackness, which are near to the chroma and value of the Munsell color system samples used in the prior experiment. Figure 5.3 is the photo of eight panels that used in this experiment.

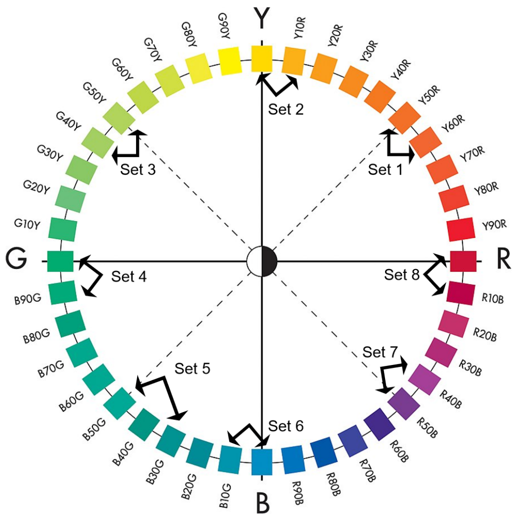

Figure 5.2: *Sample selection in NCS*

Figure 5.3: *Eight experiment panels*

During the experiment, the participants are given one minute to acclimatize to the current light. The participants were then instructed to identify the color patch with the different color as quickly as possible. Every color panel was given in a random orientation and in a random order. Also, the observation time of each panel under each light is recorded by the stopwatch. If the observer identifies the correct test color sample, the result is recorded as "True" and the time is also noted. If the individual chooses the incorrect sample or is unable to select any sample within 90 seconds, the result is recorded as "False". However, subjects were unaware of the accuracy of their responses until the end of all the experiments.

This observation session was repeated four times in random order under $L1$, $L2$, $L3$ and LW. The duration of the total experiment for one participant is around 35 minutes. After finished all the experiment, subjects were also questioned about their subjective perceptions, visual feelings and preference about each light, and they were given the opportunity to leave a comment for these lights.

5.1.3 Results

The success rate of each panel based on the results of 15 observers observing 8 panels under 4 different lighting conditions is shown in the following Table 5.1. The value in the table represents the number of correct cases, followed by the value in brackets representing the correct rate.

Table 5.1: *Success rate of four lights*

Panel	$L1$	$L2$	$L3$	LW	overall
set1	**9 (60.00%)**	8 (53.33%)	**9 (60.00%)**	3 (20.00%)	29 (48.33%)
set2	**15 (100.00%)**	**15 (100.00%)**	14 (93.33%)	14 (93.33%)	58 (96.67%)
set3	9 (60.00%)	**15 (100.00%)**	**15 (100.00%)**	12 (80.00%)	51 (85.00%)
set4	8 (53.33%)	4 (26.67%)	2 (13.33%)	**7 (46.67%)**	21 (35.00%)
set5	6 (40.00%)	**11 (73.33%)**	5 (33.33%)	6 (40.00%)	28 (46.67%)
set6	**14 (93.33%)**	**14 (93.33%)**	14 (93.33%)	10(66.67%)	52 (86.67%)
set7	13 (86.67%)	**15 (100.00%)**	**15 (100.00%)**	**15 (100.00%)**	58 (96.67%)
set8	**3 (20.00%)**	2 (13.33%)	2 (13.33%)	2 (13.33%)	9 (15.00%)
Sum	77 (64.17%)	**84 (70.00%)**	76 (63.33%)	69(57.50%)	306 (63.75%)

From the results of overall performance of every light, $L2$ has the highest rate of correct responses, while LW has the lowest success rate. The correct rate of the other two lights is similar. Additionally, it is evident from the results of each set that the number of success cases for the same panel could be vastly distinct. For instance, in set 5, eleven observers have the correct response under $L2$, while only five people can discern the difference under $L3$. Moreover, it is important to note that because the color difference between the reference sample and the test sample varies for each panel, the correct rate for each set varies greatly. The overall correct rate for each board ranged from 15% to more than 95%.

Apart from the success rate, the time is another factor that worth to be evaluated. For correct responses, a shorter response time indicates that the participant can distinguish the test sample at a glance, whereas a longer response time is associated with a slower, more detailed observation and greater uncertainty. To verify this, Figure 5.4 is the two-way independent Analysis of variance (ANOVA) box plot of the complete time of the correct answer. Most of the observations were made within 30 seconds, except for a very few extreme values. Also, the disparity between the various panels under different lighting conditions is substantial.

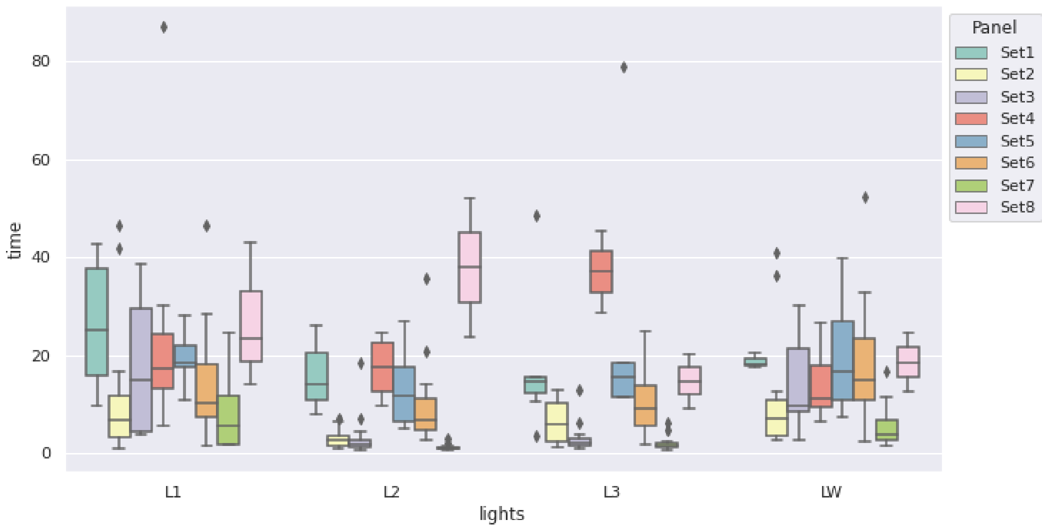

Figure 5.4: *ANOVA of time with lights and panel*

Table 5.2: *ANOVA summary*

factor	df	sum_{sq}	$mean_{sq}$	F	PR(>F)
C(panel)	7.0	10789.861726	1541.408818	15.013446	1.396857e-16
C(lights)	3.0	3102.591819	1034.197273	10.073165	2.566723e-06
Residual	274.0	28131.183967	102.668555	NaN	NaN

Table 5.2 is the summary of the ANOVA, two independent variables - light and panel being tested. The p-value of both of the panel and the light are all smaller than the significance level of 0.05, which indicates statistically significant. This suggests that the lighting influences the observation's reaction time.

The personal lighting preferences of viewers are also collected based on the subjective feelings of observers as expressed in their comments. Figure 5.5 is the pie chart that presents the observer's preference. More than 60% people prefer $L1$ and $L2$, and the most common explanation the observers give is that the color of the light appears natural. Only one participant showed a preference for LW, while two indicated they had no choice and the other two preferred $L3$. Besides, there appears to be no correlation between the illumination preferences of the observers and the correctness of their experiment results. But the smoothness of the experiment will influence the final observer's preference to some extent.

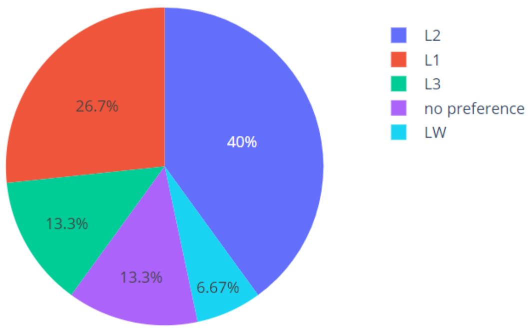

Figure 5.5: *Light preference*

5.2 Measurement

5.2.1 Method

In addition to visual differences, the color difference under different lights can also be reflected by the numerical results. In order to investigate how colors difference change, the $dE2000$ is used in this section to quantify color differences. Figure 5.6 illustrates how the $dE2000$ value was obtained. Besides the reference sample and the test sample, the XYZ value of the white reference sample is involved in the calculation from XYZ to L*a*b* for the comparison pairs in order to improve the accuracy of the results.

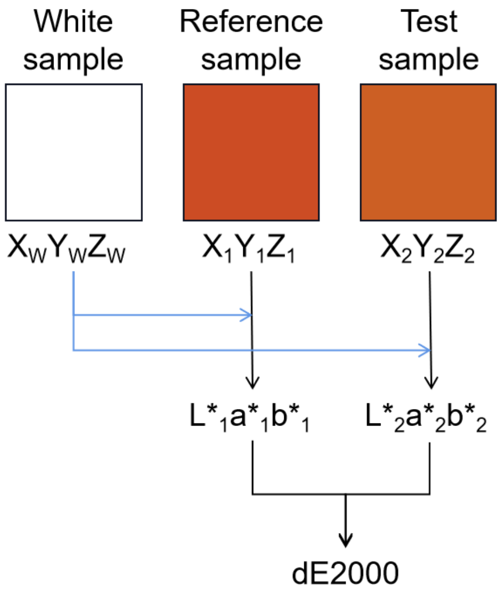

Figure 5.6: *Process of obtaining dE2000*

Because there is 1 test sample and 23 reference samples for each panel, the reference samples are selected randomly from the 23. However, during the measurement, the reference sample and test sample pairs remain the same under different lighting conditions. The color difference among all the 23 reference samples in a given panel is less than 0.02.

The measurements were performed in a room with background illumination of less than 1 lux. All the lights have the same luminance - 500 cd/m^2 for white reference sample. At the same viewing angle as the observer, the spectraval 1511 spectroradiometer (JETI, Germany) measured the XYZ values. Then the $dE2000$ color difference was calculated by MATLAB Colour Engineering Toolbox (Green and MacDonald, 2011).

5.2.2 Results

Table 5.3 shows the original $dE2000$ color difference value (under D65 lighting) of every panel and the color difference under four experiment lights. The largest color difference values in every panel among the four lights are in the bold font. The values in the brackets represent the difference between the $dE2000$ under current light and it in D65. The positive number means the color difference increases, and vice versa decreases.

Table 5.3: *Color difference under different lights*

Panel	D65	$L1$	$L2$	$L3$	LW
Set1	2.7946	2.6953(-0.0993)	2.2883(-0.5063)	2.7493(-0.0453)	**2.9639**(+0.1692)
Set2	2.9986	3.4887(+0.4901)	**4.6879**(+1.6893)	2.6384(-0.3602)	2.5359(-0.4627)
Set3	3.2805	3.1282(-0.1523)	**6.0754**(+2.7949)	5.2157(+1.9352)	3.7810(+0.5005)
Set4	2.4633	**2.4238**(-0.0395)	2.0382(-0.4251)	2.3747(-0.0886)	2.3946(-0.0687)
Set5	2.5414	2.3497(-0.1917)	**2.4877**(-0.0537)	1.8975(-0.6439)	1.9417(-0.5997)
Set6	3.6206	3.8480(+0.2274)	**4.2142**(+0.5936)	3.3777(-0.2429)	3.2127(-0.4079)
Set7	3.9066	3.4724(-0.4342)	**6.7867**(+2.8801)	6.2823(+2.3757)	3.3993(-0.5073)
Set8	1.6197	1.6628(+0.0431)	1.6903 (+0.0706)	**1.7297**(+0.1101)	1.5729 (-0.0468)

Each of these four lights has the greatest value in at least one set according to the table, but the $L2$ has the largest number of maximum color differences. Meanwhile, no light in this experiment can increase the color difference in all the set, indicating that the capability of the proposed light is hue-dependent. For example, the $L2$ has higher color difference in set5, 6 and 7, which is consistent with the results of prior psychophysical experiments. However, this could only imply that the light could help to increase the color difference in this particular hue range, but not all the other hues.

Due to the fact that the initial color difference of each set varies, in order to minimize the influence of different sets, the following ANOVA method uses the difference of $dE2000$ (values in brackets) to indicate how the color difference changes by using different lights. Figure 5.7 is the plot result. No significant differences were observed between the experiment lights in terms of increasing the color difference (p>.05).

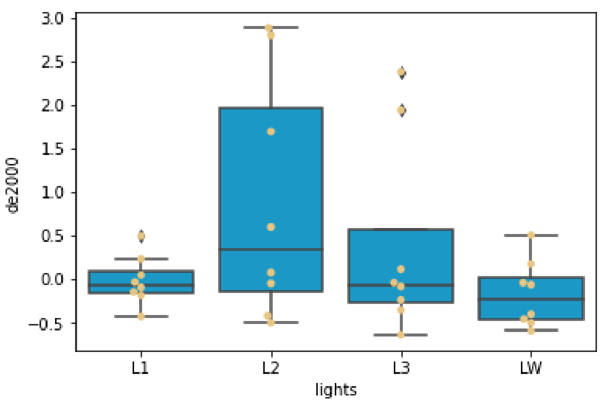

Figure 5.7: *ANOVA of color difference change*

Nevertheless, the characteristics of each light can be summed up based on the diagram and the prior findings: $L1$ has the smallest variance and the mean value is close to 0, meaning that the color difference under this light does not vary significantly. In contrast, this indicates that $L1$ has good color fidelity to preserve the color appearance; $L2$ has the largest variance and the highest mean value, as well as the best overall performance in the psychophysical experiment, so it has the potential to increase the color difference in some hue range; The variation of $L3$ is also rather big, but the mean is again close to 0. Taking into account the results of the experiment and the remarks of the observers, although $L3$ has a high fidelity and a high color gamut index, its low color temperature and distance from the Planckian locus make its visual performance unstable and unsuitable for daily interior lighting. Comparing with the proposed three lights, the reference white LED LW has lowest mean value, and does not have good performance in the experiment, which implying the multi channel LED is better than the phosphor converted white LED.

It is also worth to notice that all the $dE2000$ color difference values calculated from the XYZ values using CIE 1931 2 degree standard observer. This color difference value only represents the perception of normal healthy eyes, and cannot fully represent people with specific eye diseases.

6 | Discussion

This chapter includes observations of the experiment and some details of the process or the results that are worth discussing. Phase I and phase II correspond to the result discovery part (Chapter 4) and the result validation part (Chapter 5) respectively (See Table 4.1)

6.1 Phase I

6.1.1 Experiment

During the color arrangement experiment, all 16 participants had normal color vision; nonetheless, individual differences between observers were observed. For instance, on channel 9 (C), some observers exhibited good color discrimination with final scores all under 4, whilst the remaining observers had fairly high error scores exceeding 10. Also, for channels 12 (L) and 13 (PC-A), which are the non-narrow band light, all observers have a lower error score compared to the other channels, but only one observer has an arrangement that is entirely perfect. Therefore, the final error grade was normalized to prevent huge errors from having an effect on the results. This variation may be due to the observer's visual perception, their comprehension of the experiment, or their personality.

In addition, there are no restrictions on the arrangement methods in the experiment. Subjects were observed using a variety of methods, such as color grouping, one-by-one comparison, and making a "waiting list". Although the method used by the subject has no direct effect on the results, the method used affects the length of the experiment, which in turn affects the subject's patience. Even though the experiment was split into two halves, certain errors due to fatigue cannot be ruled out.

Also, it must be reiterated that the only variable of color in this experiment is hue. Besides this, chroma and brightness are also worth to investigate in the future.

6.1.2 Measurement

The most challenging and significant aspect of measuring every mix ratio is determining the selection criteria. However, because there is little prior literature to draw on, the coefficient and parameters in formula 4.2 are set as the possible initial values. These values necessitate a more precise iterative process backward from the experimental results.

For the three selected lights, $L2$ has the lowest color fidelity, with a CRI of only about 40 and an R_f of 66.6 according to the CIE2017 color fidelity measurements, demonstrating the limitations of CRI when evaluating LED light. Therefore, the first screening process of CRI should not be too strict to prevent missing the effective light. Also, based on the final experiment results, it is possible to conclude that the color fidelity does not significantly affect color discrimination, as the $L2$ outperformed the other lights. And the distance to the Planckian locus is noteworthy especially from the observers' comment. Consequently, the coefficient and parameters of this criterion can be modified to provide greater weight to the Duv and less weight to the color fidelity.

6.2 Phase II

6.2.1 Experiment

In the validation experiment, these three customized lights have distinct and similar properties, allowing them to be comparable. Also, additional qualities have been studied as a result of the experiment.

User experience is importance for lighting designed for low vision people. Although some people prefer warmer light like $L3$ the after-experiment session, the majority of people chose $L2$ or $L1$, which are both cold white, as their preferred lighting option. It has also been demonstrated that, compared to warm white, people prefer cool white (Khanh et al., 2018; Wang et al., 2017) and located below the Planckian locus, within the white point zone specified by CIE (Bodrogi et al., 2018; Masuda and Nascimento, 2013). $L2$ meets both of these two conditions, which makes it the most preferred light. This also demonstrates that CCT and Duv require special consideration while selecting lighting. However, as mentioned in Chapter 2, lighting preference is a very subjective matter. There is no universal standard that can be applied to everyone, but only as many as feasible.

In addition, $L1$ and $L3$ contain a non-narrow band and achieve equivalent outcomes in the experiment, but not as well as $L2$. It may indicate that the narrow band has a greater capacity to improve color discrimination since it can amplify a short range that makes colors more distinct. In subsequent studies, it suggests that narrow channels should be preferred.

Moreover, according to some observers' comments, the reflection of the samples might influence their observations, and the color of the sample can change depending on the viewing angle. Therefore, the flatness of the surface can also affect the results. This is worthy of attention that, unlike the Munsell color book, which has both the "matt" and "glossary" versions,the NCS only has a single standard album that is not completely matt. Glossiness is an influential component of color appearance, and it should be managed in future experiments to control the variables.

6.2.2 Measurement

The validation experiment has a limitation that even though the eight sample pairs were chosen as the most representative hues from the entire hue circle of NCS, they cannot reveal the accurate color discrimination abilities over the complete color range.

Also, it is difficult to control the color difference between the test sample and the reference sample in every panel to be the same. The measured $dE2000$ color difference between adjacent hue samples in the NCS album is not uniform, resulting in varying levels of difficulty for each hue pair. Particularly in the near-purple region, the color differences are more noticeable than in the other hue ranges. It is suggested that the color pair should ideally have the same color difference, which can allow evaluating the lighting capabilities in terms of increasing the color difference more objectively.

In spite of this, the experiment can demonstrate the abilities of various light characteristics to accentuate color difference. The illuminant with low Duv, high GAI, and relatively high CCT, composed of multiple narrow bands, has the potential to assist those with central vision loss to some degree.

7 | Conclusion and Future Work

7.1 Conclusion

The proposed study explores the effect of different LED lights on color discrimination and attempts to get the different combination of the LED channels to increase the color difference, which can assist low vision individuals.

Results derived from a series of psychophysical experiments and the measurements present that the variable mixture of LED can impact the color differently within a certain hue range, and it has a high correlation with response time. In addition, the remarks of observers are quite important when selecting illumination. Although the proposed lights are unable to enhance the color difference in all hue ranges, it can improve the color difference and corresponding color discrimination performance in certain hue ranges, thereby laying the groundwork for future studies. The multi-channel, narrow band, high color gamut index, and low Duv LED light has the potential to increase color difference for the benefit of those with low vision, particularly those with central loss of vision.

All of these positive and negative outcomes provide interesting and pertinent information for defining the future studies required to target more precisely the light characteristics that would be most effective in assisting low-vision individuals with mobility.

This study improves the understanding of the effect of LED lighting mixing on the color discrimination of those with impaired vision. Compare to the other visual aid approaches, the multi-channel LED lighting has the ability to increase color difference of certain hues, which can be used to assist people with central scotoma to better distinguish objects, particularly in the indoor environment.

7.2 Future Work

Based on the current existing outcomes and observations, several future researches can be conducted in the following aspects:

Firstly, the number of mixing channels can be investigated further, as the three-peak lights shown better color discrimination performance than the two-peak LED in the trial. Four or more channels of LED light mixing can be examined in a future study.

Secondly, based on the result that the proposed light can enhance color difference of a part of hue range. These hue-related improvement results also suggest that more hue pairs can be selected in the validation experiment to obtain more accurate results in terms of color discrimination of various hues.

Thirdly, with the three attributes of color being hue, saturation, and brightness, this study focuses primarily on the effect that different lights have on hue. In the following experiments, the saturation and brightness could also be investigated.

Lastly, in addition to the central scotoma, the research that would be done in the future can take into account other various muscular disorders or diseases, such as cataract, tunnel vision, and homonymous hemianopsia.

A Appendix

A.1 Lighting Channels Information

Table A.1: *Illumination information of 24 channels*

Channel	Max Luminous Flux (lm)	Peak Wavelength (nm)	FWHM (nm)
UV1	6.92	NA[a]	NA[a]
UV2	11.68	394.3	11.4
V1	28.12	407.7	13
V2	79.49	422.2	13.4
RB1	345.33	441	16.6
RB2	406.5	453	20.3
B1	721.85	468	23.7
B2	991.53	477	24.6
C	1536.27	500	28.9
G1	2392.48	516	29.4
G2	2548.00	527	31.3
L	3757.98	544	103.8
PC-A	2421.59	595	73.7
A	909.16	599	15.2
OR	2414.56	622	16.2
R1	1785.09	636	16.1
R2	822.56	654	17.2
DR1	179.49	685	18.7
DR2	33.16	709	31.3
FR1	20.03	732	28.3
FR2	1.58	765	21.2
FR3	1.64	776	20.7
IR1	0.74	870	0 35.6
IR2	0.61	958	50

[a]out of the range of measurement

A.2 Detailed Information of 3 Proposed Lights

A.2.1 CQS

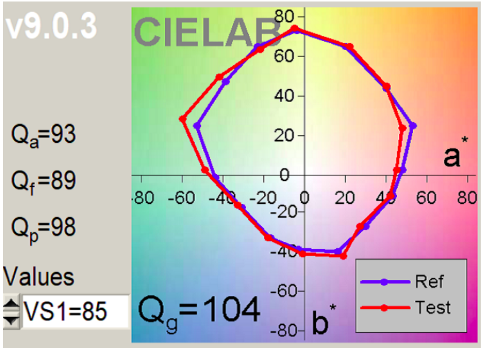

(a) *L1-CIELAB*

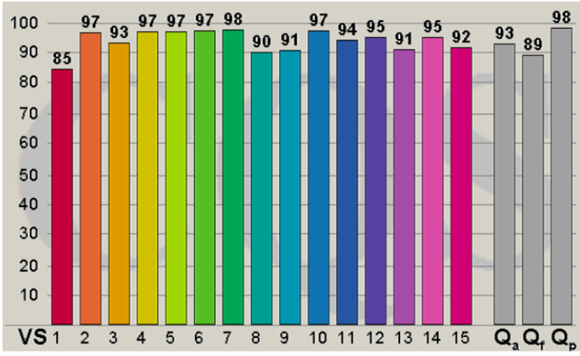

(b) *L1-CQS Columns*

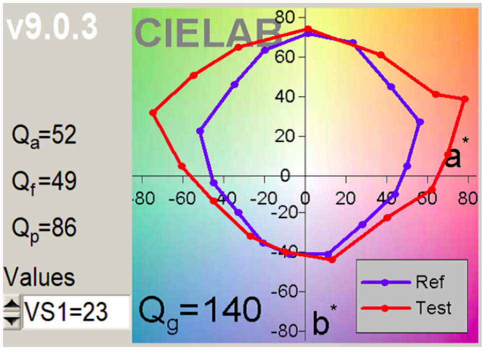

(c) *L2-CIELAB*

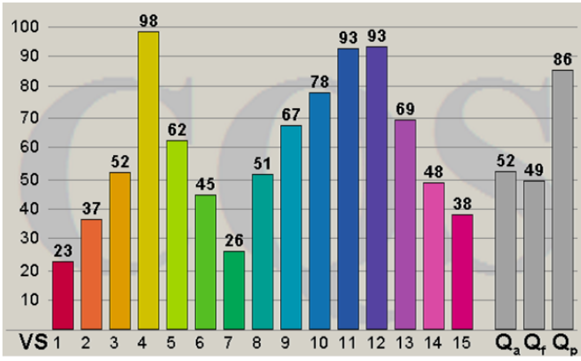

(d) *L2-CQS Columns*

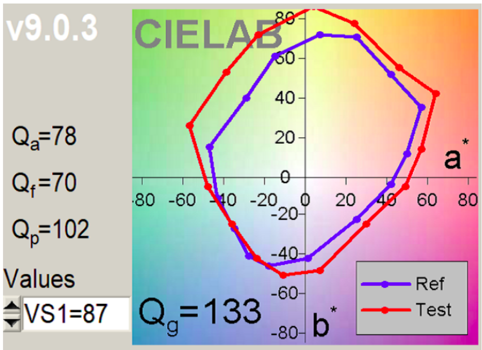

(e) *L3-CIELAB*

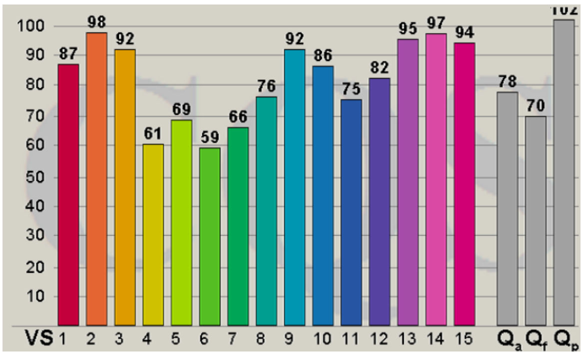

(f) *L3-CQS Columns*

Figure A.1: *CQS information of three experimental lights*

A.2.2 CIE2017 Color Fidelity Index

Rf	Rf1	Rf2	Rf3	Rf4	Rf5	Rf6	Rf7	Rf8	Rf9
90.4	97.6	96.6	85.1	92.4	83.7	97.0	86.4	80.9	95.5
Rf10	**Rf11**	**Rf12**	**Rf13**	**Rf14**	**Rf15**	**Rf16**	**Rf17**	**Rf18**	**Rf19**
92.2	95.9	96.7	87.2	98.7	96.5	88.9	98.6	96.5	96.7
Rf20	**Rf21**	**Rf22**	**Rf23**	**Rf24**	**Rf25**	**Rf26**	**Rf27**	**Rf28**	**Rf29**
69.4	92.1	97.2	97.1	96.5	87.6	99.0	89.2	94.6	98.5
Rf30	**Rf31**	**Rf32**	**Rf33**	**Rf34**	**Rf35**	**Rf36**	**Rf37**	**Rf38**	**Rf39**
93.8	95.4	93.0	97.7	97.8	98.6	78.3	90.6	88.0	89.8
Rf40	**Rf41**	**Rf42**	**Rf43**	**Rf44**	**Rf45**	**Rf46**	**Rf47**	**Rf48**	**Rf49**
79.6	97.9	82.6	80.8	98.0	84.0	92.5	90.8	94.3	87.1
Rf50	**Rf51**	**Rf52**	**Rf53**	**Rf54**	**Rf55**	**Rf56**	**Rf57**	**Rf58**	**Rf59**
86.2	85.9	78.7	82.5	93.4	93.8	93.4	92.9	93.6	94.1
Rf60	**Rf61**	**Rf62**	**Rf63**	**Rf64**	**Rf65**	**Rf66**	**Rf67**	**Rf68**	**Rf69**
94.2	91.9	90.1	88.6	95.5	88.3	96.7	98.0	93.7	90.8
Rf70	**Rf71**	**Rf72**	**Rf73**	**Rf74**	**Rf75**	**Rf76**	**Rf77**	**Rf78**	**Rf79**
92.9	78.3	96.2	84.0	92.9	74.4	88.8	88.5	79.6	93.5
Rf80	**Rf81**	**Rf82**	**Rf83**	**Rf84**	**Rf85**	**Rf86**	**Rf87**	**Rf88**	**Rf89**
92.3	87.2	96.5	97.5	92.6	82.7	82.6	91.8	97.9	89.5
Rf90	**Rf91**	**Rf92**	**Rf93**	**Rf94**	**Rf95**	**Rf96**	**Rf97**	**Rf98**	**Rf99**
96.3	67.9	74.6	87.0	76.8	80.7	91.7	92.8	95.5	91.4

Figure A.2: *L1-CIE2017 color fidelity index*

Rf	Rf1	Rf2	Rf3	Rf4	Rf5	Rf6	Rf7	Rf8	Rf9
66.6	64.3	41.6	44.6	53.5	28.0	68.2	18.0	22.0	87.0
Rf10	**Rf11**	**Rf12**	**Rf13**	**Rf14**	**Rf15**	**Rf16**	**Rf17**	**Rf18**	**Rf19**
38.6	26.2	28.9	51.2	87.5	59.5	48.3	63.2	64.9	58.8
Rf20	**Rf21**	**Rf22**	**Rf23**	**Rf24**	**Rf25**	**Rf26**	**Rf27**	**Rf28**	**Rf29**
33.9	59.2	55.6	92.4	87.4	75.0	86.9	91.9	84.4	93.9
Rf30	**Rf31**	**Rf32**	**Rf33**	**Rf34**	**Rf35**	**Rf36**	**Rf37**	**Rf38**	**Rf39**
86.1	94.0	82.5	92.8	74.4	80.3	80.0	58.1	94.0	88.5
Rf40	**Rf41**	**Rf42**	**Rf43**	**Rf44**	**Rf45**	**Rf46**	**Rf47**	**Rf48**	**Rf49**
75.3	94.7	36.6	52.1	97.8	50.3	59.1	79.5	47.4	62.7
Rf50	**Rf51**	**Rf52**	**Rf53**	**Rf54**	**Rf55**	**Rf56**	**Rf57**	**Rf58**	**Rf59**
67.9	70.4	60.3	56.4	68.6	74.3	62.8	63.8	65.0	73.0
Rf60	**Rf61**	**Rf62**	**Rf63**	**Rf64**	**Rf65**	**Rf66**	**Rf67**	**Rf68**	**Rf69**
93.4	77.3	95.9	91.7	69.8	67.3	80.8	82.8	80.1	79.6
Rf70	**Rf71**	**Rf72**	**Rf73**	**Rf74**	**Rf75**	**Rf76**	**Rf77**	**Rf78**	**Rf79**
89.2	92.1	96.0	88.6	90.6	83.7	76.1	79.2	78.6	85.3
Rf80	**Rf81**	**Rf82**	**Rf83**	**Rf84**	**Rf85**	**Rf86**	**Rf87**	**Rf88**	**Rf89**
68.6	63.8	90.7	90.1	67.7	62.7	28.2	39.8	42.4	59.2
Rf90	**Rf91**	**Rf92**	**Rf93**	**Rf94**	**Rf95**	**Rf96**	**Rf97**	**Rf98**	**Rf99**
49.2	64.5	30.8	52.4	42.0	38.7	49.8	47.9	53.4	23.1

Figure A.3: *L2-CIE2017 color fidelity index*

Rf	Rf1	Rf2	Rf3	Rf4	Rf5	Rf6	Rf7	Rf8	Rf9
80.5	84.3	76.7	79.6	85.5	76.9	92.7	65.9	72.2	93.2
Rf10	Rf11	Rf12	Rf13	Rf14	Rf15	Rf16	Rf17	Rf18	Rf19
83.4	86.9	81.8	80.2	96.8	86.1	84.0	89.9	88.8	92.5
Rf20	Rf21	Rf22	Rf23	Rf24	Rf25	Rf26	Rf27	Rf28	Rf29
48.1	86.2	83.7	91.3	81.3	77.3	76.1	92.9	82.7	69.0
Rf30	Rf31	Rf32	Rf33	Rf34	Rf35	Rf36	Rf37	Rf38	Rf39
84.8	68.7	57.6	75.8	65.8	79.2	91.5	65.0	88.2	90.9
Rf40	Rf41	Rf42	Rf43	Rf44	Rf45	Rf46	Rf47	Rf48	Rf49
82.3	86.7	54.4	54.4	98.0	64.5	70.2	72.1	71.9	68.4
Rf50	Rf51	Rf52	Rf53	Rf54	Rf55	Rf56	Rf57	Rf58	Rf59
79.8	82.2	76.8	71.2	85.0	88.0	77.7	77.7	78.0	89.6
Rf60	Rf61	Rf62	Rf63	Rf64	Rf65	Rf66	Rf67	Rf68	Rf69
97.7	95.3	96.9	93.1	90.7	88.7	92.8	92.4	91.0	84.0
Rf70	Rf71	Rf72	Rf73	Rf74	Rf75	Rf76	Rf77	Rf78	Rf79
83.6	81.4	93.1	75.7	89.7	78.6	67.3	80.3	67.6	87.6
Rf80	Rf81	Rf82	Rf83	Rf84	Rf85	Rf86	Rf87	Rf88	Rf89
77.2	82.9	90.5	86.6	82.9	81.3	71.5	69.1	73.3	80.8
Rf90	Rf91	Rf92	Rf93	Rf94	Rf95	Rf96	Rf97	Rf98	Rf99
76.0	77.3	73.8	81.2	82.9	73.2	77.4	74.0	77.9	68.5

Figure A.4: *L3-CIE2017 color fidelity index*

Bibliography

Aguerrevere, D., Choudhury, M., and Barreto, A. (2004). Portable 3d sound/sonar navigation system for blind individuals. In *2nd LACCEI Int. Latin Amer. Caribbean Conf. Eng. Technol. Miami, FL*. Citeseer. (cited on page 18)

Aladren, A., López-Nicolás, G., Puig, L., and Guerrero, J. J. (2014). Navigation assistance for the visually impaired using rgb-d sensor with range expansion. *IEEE Systems Journal*, 10(3):922–932. (cited on page 18)

Almutleb, E. S. and Hassan, S. E. (2020). The effect of simulated central field loss on street-crossing decision-making in young adult pedestrians. *Optometry and vision science: official publication of the American Academy of Optometry*, 97(4):229. (cited on page 9)

Azuma, R., Baillot, Y., Behringer, R., Feiner, S., Julier, S., and MacIntyre, B. (2001). Recent advances in augmented reality. *IEEE computer graphics and applications*, 21(6):34–47. (cited on page 19)

Bai, J., Lian, S., Liu, Z., Wang, K., and Liu, D. (2017). Smart guiding glasses for visually impaired people in indoor environment. *IEEE Transactions on Consumer Electronics*, 63(3):258–266. (cited on page 18)

Bao, J., Song, X., Li, Y., Bai, Y., and Zhou, Q. (2021). Effect of lighting illuminance and colour temperature on mental workload in an office setting. *Scientific reports*, 11(1):1–10. (cited on page 15)

Baraas, R. C., Kremers, J., and Marshall, N. J. (2018). *Human Color Vision*. Springer. (cited on page 4)

Bhatlawande, S., Mahadevappa, M., Mukherjee, J., Biswas, M., Das, D., and Gupta, S. (2014). Design, development, and clinical evaluation of the electronic mobility cane for vision rehabilitation. *IEEE Transactions on Neural Systems and Rehabilitation Engineering*, 22(6):1148–1159. (cited on page 18)

Bodrogi, P., Guo, X., Stojanovic, D., Fischer, S., and Khanh, T. Q. (2018). Observer preference for perceived illumination chromaticity. *Color Research & Application*, 43(4):506–516. (cited on page 46)

Bourne, R., Steinmetz, J. D., Flaxman, S., Briant, P. S., Taylor, H. R., Resnikoff, S., Casson, R. J., Abdoli, A., Abu-Gharbieh, E., Afshin, A., et al. (2021). Trends in prevalence of blindness and distance and near vision impairment over 30 years: an analysis for the global burden of disease study. *The Lancet global health*, 9(2):e130–e143. (cited on page 7)

Brunnström, G., Sörensen, S., Alsterstad, K., and Sjöstrand, J. (2004). Quality of light and quality of life–the effect of lighting adaptation among people with low vision. *Ophthalmic and Physiological Optics*, 24(4):274–280. (cited on page 20)

Butler, M., McMullan, K., and Ryan, S. E. (2019). Lighting prescriptions for low vision. *Journal of Housing for the Elderly*, 33(2):189–203. (cited on page 10)

Carmigniani, J., Furht, B., Anisetti, M., Ceravolo, P., Damiani, E., and Ivkovic, M. (2011). Augmented reality technologies, systems and applications. *Multimedia tools and applications*, 51(1):341–377. (cited on page 19)

CIE (2007). *Color Rendering of White LED Light Sources*. Technical Report CIE 177:2007. (cited on page 32)

CIE (2017). *Lighting for older people and people with visual impairment in buildings*. Technical Report CIE 227:2017. (cited on page 10)

CIE, I. (1987). International lighting vocabulary. *Central Bureau ofthe Commission Internationale de l'Eclairage, Kegelgasse*, 27. (cited on page 13)

CIE 117-1995 (1995). Discomfort Glare in Interior Lighting. Standard, Commission International de l'Eclairage. (cited on page 15)

CIE 190:2010 (2010). Calculation and Presentation of Unified Glare Rating Tables of Indoor Lighting. Standard, International Commission on Illumination, Vienna: Commission International de l'Eclairage. (cited on page 10)

CIE 224:2017 (2017). Color fidelity index for accurate scientific use. Standard, Commission International de l'Eclairage. (cited on page 14)

Clinic, M. (2009). *Mayo Clinic Family Health Book*. Little Brown & Co, 5 edition. (cited on page 8)

Copolillo, A., Christopher, A., and Lyons, A. (2017). Effects of simulated low vision on postural adjustment to changes in center of mass in older adults. *Occupational Therapy In Health Care*, 31(2):115–125. (cited on page 9)

Corn, A. L. and Erin, J. N. (2010). *Foundations of low vision: Clinical and functional perspectives*. American Foundation for the Blind. (cited on page 6)

Culham, L. E., Chabra, A., and Rubin, G. S. (2004). Clinical performance of electronic, head-mounted, low-vision devices. *Ophthalmic and Physiological Optics*, 24(4):281–290. (cited on page 19)

Dakopoulos, D. and Bourbakis, N. (2008). Preserving visual information in low resolution images during navigation of visually impaired. In *Proceedings of the 1st international conference on PErvasive Technologies Related to Assistive Environments*, pages 1–6. (cited on page 18)

Davis, W. and Ohno, Y. (2010). Color quality scale. *Optical engineering*, 49(3):033602. (cited on page 14)

Ehrlich, J. R., Ojeda, L. V., Wicker, D., Day, S., Howson, A., Lakshminarayanan, V., and Moroi, S. E. (2017). Head-mounted display technology for low-vision rehabilitation and vision enhancement. *American journal of ophthalmology*, 176:26–32. (cited on page 19)

Evans, B., Sawyerr, H., Jessa, Z., Brodrick, S., and Slater, A. (2010). A pilot study of lighting and low vision in older people. *Lighting Research & Technology*, 42(1):103–119. (cited on pages 10 and 20)

Farnsworth, D. (1943). The farnsworth-munsell 100-hue and dichotomous tests for color vision. *JOSA*, 33(10):568–578. (cited on page 27)

Findlater, L. and McGrenere, J. (2004). A comparison of static, adaptive, and adaptable menus. In *Proceedings of the SIGCHI conference on Human factors in computing systems*, pages 89–96. (cited on page 19)

García, A., Fonseca, R., and Durán, A. (2011). Electronic long cane for locomotion improving on visual impaired people. a case study. In *2011 Pan American health care exchanges*, pages 58–61. IEEE. (cited on page 18)

Gopalakrishnan, S., Muralidharan, A., Susheel, S. C., and Raman, R. (2017). Improvement in distance and near visual acuities using low vision devices in diabetic retinopathy. *Indian journal of ophthalmology*, 65(10):995. (cited on page 19)

Gopalakrishnan, S., Suwalal, S. C., Bhaskaran, G., and Raman, R. (2020). Use of augmented reality technology for improving visual acuity of individuals with low vision. *Indian Journal of Ophthalmology*, 68(6):1136. (cited on page 19)

Gordon, G. (2015). *Interior lighting for designers*. John Wiley & Sons. (cited on page 10)

Górnicka, G. (2008). Lighting at work: Environmental study of direct effects of lighting level and spectrum on psychophysiological variables. (cited on page 10)

Green, P. and MacDonald, L. (2011). *Colour engineering: achieving device independent colour*. John Wiley & Sons. (cited on page 41)

Haymes, S. A. and Lee, J. (2006). Effects of task lighting on visual function in age-related macular degeneration. *Ophthalmic and Physiological Optics*, 26(2):169–179. (cited on page 10)

Hegde, A. L. and Rhodes, R. (2010). Assessment of lighting in independent living facilities and residents' perceptions. *Journal of applied gerontology*, 29(3):381–390. (cited on page 10)

Henry, R., Duquette, J., and Wittich, W. (2020). Comparison of two lighting assessment methods when reading with low vision. *Optometry and Vision Science*, 97(4):257–264. (cited on page 20)

Hossain, E., Khan, M. R., Muhida, R., and Ali, A. (2011). State of the art review on walking support system for visually impaired people. *International Journal of Biomechatronics and Biomedical Robotics*, 1(4):232–251. (cited on page 18)

Huang, J., Kinateder, M., Dunn, M. J., Jarosz, W., Yang, X.-D., and Cooper, E. A. (2019). An augmented reality sign-reading assistant for users with reduced vision. *PloS one*, 14(1):e0210630. (cited on page 19)

Hurvich, L. M. and Jameson, D. (1957). An opponent-process theory of color vision. *Psychological review*, 64(6p1):384. (cited on page 5)

Hwang, A. D. and Peli, E. (2014). An augmented-reality edge enhancement application for google glass. *Optometry and vision science: official publication of the American Academy of Optometry*, 91(8):1021. (cited on page 19)

Hye Oh, J., Ji Yang, S., and Rag Do, Y. (2014). Healthy, natural, efficient and tunable lighting: four-package white leds for optimizing the circadian effect, color quality and vision performance. *Light: Science & Applications*, 3(2):e141–e141. (cited on page 15)

IEC 60050-845:1987 (2012). International Electrotechnical Vocabulary: Luminous efficacy of radiation (for a specified photometric condition). 845-21-090, International Electrotechnical Commission(IEC). (cited on page 13)

Islam, M. M., Sadi, M. S., Zamli, K. Z., and Ahmed, M. M. (2019). Developing walking assistants for visually impaired people: A review. *IEEE Sensors Journal*, 19(8):2814–2828. (cited on pages 17 and 18)

ISO 13586:2000E (2002). Lighting of work places — Part 1: Indoor. Standard, International Organization for Standardization, Vienna: Commission International de l'Eclairage. (cited on page 10)

Ito, K., Okamoto, M., Akita, J., Ono, T., Gyobu, I., Takagi, T., Hoshi, T., and Mishima, Y. (2005). Cyarm: an alternative aid device for blind persons. In *CHI'05 extended abstracts on human factors in computing systems*, pages 1483–1488. (cited on page 18)

Jager, R. D., Mieler, W. F., and Miller, J. W. (2008). Age-related macular degeneration. *New England Journal of Medicine*, 358(24):2606–2617. (cited on page 8)

Jeong, G.-Y. and Yu, K.-H. (2016). Multi-section sensing and vibrotactile perception for walking guide of visually impaired person. *Sensors*, 16(7):1070. (cited on page 18)

Jost, S., Cauwerts, C., and Avouac, P. (2018). Cie 2017 color fidelity index rf: a better index to predict perceived color difference? *JOSA A*, 35(4):B202–B213. (cited on page 14)

Kammoun, S., Parseihian, G., Gutierrez, O., Brilhault, A., Serpa, A., Raynal, M., Oriola, B., Macé, M.-M., Auvray, M., Denis, M., et al. (2012). Navigation and space perception assistance for the visually impaired: The navig project. *Irbm*, 33(2):182–189. (cited on page 18)

Kang, M.-C., Chae, S.-H., Sun, J.-Y., Lee, S.-H., and Ko, S.-J. (2017). An enhanced obstacle avoidance method for the visually impaired using deformable grid. *IEEE Transactions on Consumer Electronics*, 63(2):169–177. (cited on page 18)

Katemake, P., Radsamrong, A., Dinet, É., Heng, C. W., Kuang, Y. C., Kalavally, V., and Trémeau, A. (2019). Influence of led-based assistive lighting solutions on the autonomous mobility of low vision people. *Building and Environment*, 157:172–184. (cited on page 20)

Khanh, T., Bodrogi, P., Vinh, Q., Guo, X., and Anh, T. (2018). Colour preference, naturalness, vividness and colour quality metrics, part 4: Experiments with still life arrangements at different correlated colour temperatures. *Lighting Research & Technology*, 50(6):862–879. (cited on page 46)

Kofod, C. (2017). Indoor lighting in the public and private service sectors. *Guidelines for Indoor Lighting in the Public and Private Service Sector*, pages 1–56. (cited on page 35)

Kruisselbrink, T., Dangol, R., and Rosemann, A. (2018). Photometric measurements of lighting quality: An overview. *Building and Environment*, 138:42–52. (cited on page 11)

Kruithof, A. A. (1941). Tubular luminescence lamps for general illumination. *Philips Technical Review*, 6:65–96. (cited on page 10)

kumar Krishnan, A., Queener, H. M., Stevenson, S. B., Benoit, J. S., and Bedell, H. E. (2019). Impact of simulated micro-scotomas on reading performance in central and peripheral retina. *Experimental eye research*, 183:9–19. (cited on page 9)

Lane, J., Robbins, R. A., Rohan, E. M., Crookes, K., Essex, R. W., Maddess, T., Sabeti, F., Mazlin, J.-L., Irons, J., Gradden, T., et al. (2019). Caricaturing can improve facial expression recognition in low-resolution images and age-related macular degeneration. *Journal of Vision*, 19(6):18–18. (cited on page 9)

Leat, S. J., Legge, G. E., and Bullimore, M. (1999). What is low vision. *Optom Vis Sci*, 76:198–211. (cited on page 6)

Lee, D. A. and Higginbotham, E. J. (2005). Glaucoma and its treatment: a review. *American journal of health-system pharmacy*, 62(7):691–699. (cited on page 8)

Lim, L. S., Mitchell, P., Seddon, J. M., Holz, F. G., and Wong, T. Y. (2012). Age-related macular degeneration. *The Lancet*, 379(9827):1728–1738. (cited on page 8)

Lorenzini, M.-C. and Wittich, W. (2020). Factors related to the use of magnifying low vision aids: a scoping review. *Disability and Rehabilitation*, 42(24):3525–3537. (cited on page 19)

Lutz, W., Sanderson, W., and Scherbov, S. (2008). The coming acceleration of global population ageing. *Nature*, 451(7179):716–719. (cited on page 1)

Macnamara, A., Chen, C., Schinazi, V. R., Saredakis, D., and Loetscher, T. (2021). Simulating macular degeneration to investigate activities of daily living: A systematic review. *Frontiers in Neuroscience*, page 1026. (cited on page 9)

Masuda, O. and Nascimento, S. M. (2013). Best lighting for naturalness and preference. *Journal of Vision*, 13(7):4–4. (cited on page 46)

Meers, S. and Ward, K. (2005). A vision system for providing the blind with 3d colour perception of the environment. (cited on page 18)

Meers, S. and Ward, K. (2010). Head-tracking haptic computer interface for the blind. *in Advances in Haptics, INTECH*, pages 143–154. (cited on page 18)

Meijer, P. B. (1992). An experimental system for auditory image representations. *IEEE transactions on biomedical engineering*, 39(2):112–121. (cited on page 18)

Mekhalfi, M. L., Melgani, F., Zeggada, A., De Natale, F. G., Salem, M. A.-M., and Khamis, A. (2016). Recovering the sight to blind people in indoor environments with smart technologies. *Expert systems with applications*, 46:129–138. (cited on page 18)

Milgram, P. and Kishino, F. (1994). A taxonomy of mixed reality visual displays. *IEICE TRANSACTIONS on Information and Systems*, 77(12):1321–1329. (cited on page 19)

Millodot, M. (2014). *Dictionary of Optometry and Visual Science E-Book*. Elsevier Health Sciences. (cited on page 6)

Oh, J. H., Yoo, H., Park, H. K., and Do, Y. R. (2015). Analysis of circadian properties and healthy levels of blue light from smartphones at night. *Scientific reports*, 5(1):1–9. (cited on page 15)

O'Brien, E. E., Mohtar, A. A., Diment, L. E., and Reynolds, K. J. (2014). A detachable electronic device for use with a long white cane to assist with mobility. *Assistive Technology*, 26(4):219–226. (cited on page 18)

Park, N.-K. and Farr, C. A. (2007). The effects of lighting on consumers' emotions and behavioral intentions in a retail environment: A cross-cultural comparison. *Journal of Interior Design*, 33(1):17–32. (cited on page 10)

Pimputkar, S., Speck, J. S., DenBaars, S. P., and Nakamura, S. (2009). Prospects for led lighting. *Nature photonics*, 3(4):180–182. (cited on page 22)

Rao, G. N., Khanna, R., and Payal, A. (2011). The global burden of cataract. *Current opinion in ophthalmology*, 22(1):4–9. (cited on page 8)

Rea, M. S. (2010). A practical and predictive two-metric system for characterizing the color rendering properties of light sources used for architectural applications. In *International Optical Design Conference*, page IMB1. Optica Publishing Group. (cited on page 31)

Ringering, L. and Amaral, P. (2000). The role of psychosocial factors in adaptation to vision impairment and rehabilitation outcomes for adults and older adults. *The Lighthouse handbook on vision impairment and vision rehabilitation*, 1:1029–1048. (cited on page 19)

Rolland, J. P. and Hua, H. (2005). Head-mounted display systems. *Encyclopedia of optical engineering*, 2. (cited on page 19)

Rotruck, J., Fletcher, D. C., and Walker, L. (2015). Low vision patients with amd and poag may require different lighting to maximize visual acuity. *Investigative Ophthalmology & Visual Science*, 56(7):4792–4792. (cited on page 20)

Sa-Ngadsup, P., Dinet, E., Katemake, P., and Trémeau, A. (2018). Using light to facilitate the mobility of low vision people. In *Topical Conference on Smart Lighting*, pages 181–190. International Commission on Illumination (CIE). (cited on page 20)

Salat, S. and Habib, M. A. (2019). Smart electronic cane for the assistance of visually impaired people. In *2019 IEEE International WIE Conference on Electrical and Computer Engineering (WIECON-ECE)*, pages 1–4. IEEE. (cited on page 18)

Sandnes, F. E. and Eika, E. (2017). Head-mounted augmented reality displays on the cheap: a diy approach to sketching and prototyping low-vision assistive technologies. In *International Conference on Universal Access in Human-Computer Interaction*, pages 167–186. Springer. (cited on page 19)

Sawyer, J. and Kaup, M. L. (2014). Lighting, vision, and aging in place: the impact of living with low vision in independent living facilities. *Undergraduate Research Journal for the Human Sciences*, 13(1). (cited on page 7)

Scott, I. U., Smiddy, W. E., Schiffman, J., Feuer, W. J., and Pappas, C. J. (1999). Quality of life of low-vision patients and the impact of low-vision services. *American journal of ophthalmology*, 128(1):54–62. (cited on page 7)

Shoval, S., Ulrich, I., and Borenstein, J. (2003). Robotics-based obstacle-avoidance systems for the blind and visually impaired. *IEEE Robotics Magazine*, 10(1):9–20. (cited on page 18)

Sinoo, M. M., Van Hoof, J., and Kort, H. S. (2011). Light conditions for older adults in the nursing home: Assessment of environmental illuminances and colour temperature. *Building and Environment*, 46(10):1917–1927. (cited on page 10)

Söveny, B., Kovács, G., and Kardkovács, Z. T. (2014). Blind guide-a virtual eye for guiding indoor and outdoor movement. In *2014 5th IEEE Conference on Cognitive Infocommunications (CogInfoCom)*, pages 343–347. IEEE. (cited on page 18)

Stearns, L., DeSouza, V., Yin, J., Findlater, L., and Froehlich, J. E. (2017). Augmented reality magnification for low vision users with the microsoft hololens and a finger-worn camera. In *Proceedings of the 19th International ACM SIGACCESS Conference on Computers and Accessibility*, pages 361–362. (cited on page 19)

Stearns, L., Findlater, L., and Froehlich, J. E. (2018). Design of an augmented reality magnification aid for low vision users. In *Proceedings of the 20th international ACM SIGACCESS conference on computers and accessibility*, pages 28–39. (cited on page 19)

Steinmetz, J. D., Bourne, R. R., Briant, P. S., Flaxman, S. R., Taylor, H. R., Jonas, J. B., Abdoli, A. A., Abrha, W. A., Abualhasan, A., Abu-Gharbieh, E. G., et al. (2021). Causes of blindness and vision impairment in 2020 and trends over 30 years, and prevalence of avoidable blindness in relation to vision 2020: the right to sight: an analysis for the global burden of disease study. *The Lancet Global Health*, 9(2):e144–e160. (cited on page 8)

Stelmack, J. (2001). Quality of life of low-vision patients and outcomes of low-vision rehabilitation. *Optometry and Vision Science*, 78(5):335–342. (cited on page 7)

Tham, Y.-C., Li, X., Wong, T. Y., Quigley, H. A., Aung, T., and Cheng, C.-Y. (2014). Global prevalence of glaucoma and projections of glaucoma burden through 2040: a systematic review and meta-analysis. *Ophthalmology*, 121(11):2081–2090. (cited on page 1)

Turid Borgestrand, Ø. (2021). Universal design and low-vision rehabilitation: The case for a holistic lighting assessment. *Universal Design 2021: From Special to Mainstream Solutions*, 282:288. (cited on page 20)

Ulrich, I. and Borenstein, J. (2001). The guidecane-applying mobile robot technologies to assist the visually impaired. *IEEE Transactions on Systems, Man, and Cybernetics-Part A: Systems and Humans*, 31(2):131–136. (cited on page 18)

van Nispen, R. M., Virgili, G., Hoeben, M., Langelaan, M., Klevering, J., Keunen, J. E., and van Rens, G. H. (2020). Low vision rehabilitation for better quality of life in visually impaired adults. *Cochrane Database of Systematic Reviews*, (1). (cited on page 7)

Wang, Q., Xu, H., Zhang, F., and Wang, Z. (2017). Influence of color temperature on comfort and preference for led indoor lighting. *Optik*, 129:21–29. (cited on page 46)

WHO (2018). Icd-11 for mortality and morbidity statistics (2018). (cited on page 6)

WHO (2019). *World Report on Vision.* Licence: CC BY-NC-SA 3.0 IGO. (cited on page 4)

WHO (2021). Blindness and vision impairment. `https://www.who.int/en/news-room/fact-sheets/detail/blindness-and-visual-impairment`. Accessed: 2022-04-04. (cited on pages 7, 8, and 19)

Wittich, W., Amour, L. S., Jarry, J., and Seiple, W. (2018). Test-retest variability of a standardized low vision lighting assessment. *Optometry and Vision Science*, 95(9):852. (cited on page 20)

Wong, W. L., Su, X., Li, X., Cheung, C. M. G., Klein, R., Cheng, C.-Y., and Wong, T. Y. (2014). Global prevalence of age-related macular degeneration and disease burden projection for 2020 and 2040: a systematic review and meta-analysis. *The Lancet Global Health*, 2(2):e106–e116. (cited on page 1)

WPP (2019). United nations, department of economic and social affairs, population division. world population prospects 2019: Highlights (st/esa/ser. a/423). (cited on pages 1 and 7)

Wu, H., Ashmead, D. H., Adams, H., and Bodenheimer, B. (2018). Using virtual reality to assess the street crossing behavior of pedestrians with simulated macular degeneration at a roundabout. *Frontiers in ICT*, page 27. (cited on page 9)

Yam, J. and Kwok, A. K. (2014). Ultraviolet light and ocular diseases. *International ophthalmology*, 34(2):383–400. (cited on page 23)

Yang, K., Wang, K., Bergasa, L. M., Romera, E., Hu, W., Sun, D., Sun, J., Cheng, R., Chen, T., and López, E. (2018). Unifying terrain awareness for the visually impaired through real-time semantic segmentation. *Sensors*, 18(5):1506. (cited on page 18)

Yang, K., Wang, K., Hu, W., and Bai, J. (2016). Expanding the detection of traversable area with realsense for the visually impaired. *Sensors*, 16(11):1954. (cited on page 18)

Zagar, M. and Baggarly, S. (2010). Low vision simulator goggles in pharmacy education. *American journal of pharmaceutical education*, 74(5). (cited on page 9)

Zelek, J., Audette, R., Balthazaar, J., and Dunk, C. (1999). A stereo-vision system for the visually impaired. *University of Guelph*, 1999. (cited on page 18)

Zhao, Y., Szpiro, S., and Azenkot, S. (2015). Foresee: A customizable head-mounted vision enhancement system for people with low vision. In *Proceedings of the 17th international ACM SIGACCESS conference on computers & accessibility*, pages 239–249. (cited on page 19)

List of Figures

List of Tables